12-2008

Urinary Excretion of (1-3)-Beta-D-Glucans.

Debra K. Head
East Tennessee State University

Urinary Excretion of (1-3)-Beta-D-Glucans

A thesis

presented to

the faculty of the Department of Pharmacology

East Tennessee State University

In partial fulfillment

of the requirements for the degree

Master of Science in Biomedical Sciences

---

by

Debra K Head

December 2008

Peter J. Rice, Pharm.D., Ph.D., Chair

Kenneth E. Ferslew, Ph.D.

Thomas W. Ecay, Ph.D.

David L. Williams, Ph.D.

Keywords: Glucan, Fungal PAMP, Pharmacokinetics, Renal Excretion, Immunopharmacology

ABSTRACT

Urinary Excretion of (1→3)-β-D-Glucans

by

Debra K Head

(1→3)-β-D-Glucans are carbohydrate polymers that are present in the cell wall of various fungi and bacteria; they are pathogen associated molecular patterns that circulate during infection and modulate immunity. Our laboratory has previously established the pharmacokinetics of intravenously and orally administered glucans; the present studies investigated the renal excretion of (1→3)-β-D-glucans following intravenous and oral administration. Three fluorescently-labeled glucans were administered to adult male rats in the presence or absence of toxic challenge. Urine specimens were collected and analyzed by fluorescence spectroscopy, size-exclusion chromatography and GPC/MALLS. 71 ± 3% of fluorescence remained in the >5K MWCO fraction; this fraction showed a minor peak with a molecular mass (171 ± 11K) corresponding to injected glucan (~150K). Most excreted glucans were of lower molecular mass (13 ± 8.5K), indicating most (1→3)-β-D-glucans are excreted by the kidneys as smaller polysaccharides. The presence of urinary glucans may be an important indicator of fungal infection.

DEDICATION

To my parents, Greg and Gina Head, who have loved and supported me unconditionally.

To my closest friend, Stuart Large, who has encouraged me, prayed for me, motivated me and supported me in my pursuit of this degree and in every other aspect of life.

And to my Lord, Jesus Christ, in whom everything is possible. Without His love and grace, I could not live. He is the reason I am here.

"Now to Him who is able to do immeasurably more than we ask or imagine, according to His power that is at work within us, to him be glory in the church and in Christ Jesus throughout all generations, for ever and ever! Amen."

Ephesians 3:20

ACKNOWLEDGEMENTS

I would like to show gratitude to my research supervisor and mentor, Dr. Peter Rice, for his advice, his help in experimental design and data analysis, his writing tips, and the financial support he provided through my assistantship with his laboratory. I am deeply indebted for all he has done, and I wish him luck in his future pursuits.

My committee members, Dr. Kenneth Ferslew, Dr. Thomas Ecay, and Dr. David Williams, were instrumental in planning my research and thesis and in approving my work!

I owe many thanks to my coworkers who contributed significantly, whether in aiding with experiments, providing insight or troubleshooting: Dr. Tammy Ozment-Skelton, Janet Lightner, and Bridget Graves.

I would like to thank Dr. Greg Hanley and the staff of the Department of Laboratory Animal Resources for their valuable assistance with my animal studies.

Dr. Mitchell Robinson and Beverly Sherwood of the Biomedical Sciences program have been very flexible and helpful, and I am grateful to them for giving me this opportunity.

Last but not least, I would like to acknowledge my undergraduate advisor and friend, Dr. Karen Kelly, who has been a constant source of advice and encouragement throughout my undergraduate and graduate education.

My research was supported by a grant from J.Pharma.

CONTENTS

LIST OF TABLES

LIST OF FIGURES

Figure Page

CHAPTER 1

INTRODUCTION

Overview of Renal Function

All living organisms require some method of balancing nutrients and water obtained from their food sources while excreting waste, or unnecessary substances, along with water. In most animals, this method is the renal system. The kidneys are the main component of the renal system; their function is to filter, reabsorb, and secrete water and nutrients between the peritubular blood vessels and the nephron to maintain homeostasis. Under normal conditions in humans, approximately 1200 mL of blood passes through kidneys every minute, which is equal to 20% of the total cardiac output. Of that, 650 mL/min is plasma. Approximately 20% of this plasma flow is filtered into the nephron, amounting to 180 L/day of filtered plasma at a glomerular filtration rate (GFR) of 125 mL/min (Costanzo 2006). It is evident from these statistics that the kidneys are essential for filtering the blood in our systems.

There are three major processes that occur within the nephron. First, filtration occurs between the glomerular capillaries and Bowman's capsule of the nephron. During this process, plasma is filtered into the nephron (according to the GFR mentioned above), containing all but the molecules with the highest molecular weights. The unfiltered plasma continues from the glomerular capillary into the efferent arteriole, which leads to the peritubular capillaries. Here, the second process of reabsorption takes place. The vast majority of the water and nutrients that were filtered into the nephron are reabsorbed back into the peritubular capillaries; for many substances, this occurs at a rate of 99% or more reabsorption and is an energy-dependent process, using active transport mechanisms. Sodium is the primary ion reabsorbed along the

nephron; it is vital in maintaining fluid balance, and in turn, normal blood pressure and volume. Within the peritubular capillaries, secretion can also take place, which is the third process. The main purpose of secretion is to rid the unfiltered plasma fraction of waste products and unneeded substances, which are then excreted as urine (Costanzo 2006).

Fluid balance in the kidneys is driven by osmotic and hydrostatic pressures, collectively referred to as Starling forces. These pressures are responsible for equilibrium between net filtration and net reabsorption of substances within the vasculature of the kidney; however, Starling forces are also responsible for the interdependent high filtration rate at the glomerular capillary and high reabsorption rate at the peritubular capillary. The membrane sodium gradient and electrochemical gradient also play a role in regulating reabsorption and secretion; the sodium-potassium ATPase (Na/K ATPase) is the major force driving the transport of all other substances in the kidney (Costanzo 2006).

There are different segments within the nephron; each segment has a unique cell type with various transport mechanisms. The early proximal tubule cells contain Na^+ co-transporters specific for glucose, amino acids, and phosphate/lactate/citrate, as well as a Na^+/H^+ antiporter; these are all driven by the primary active transporter Na^+/K^+ ATPase. Approximately 99% of filtered glucose and amino acids are reabsorbed in this segment. The late proximal tubule cells contain parallel sodium-proton (Na^+/H^+) and chlorine-base (Cl^-/Base) antiporters that result in paracellular reabsorption of Cl^-, which brings with it cations such as Na^+, Ca^{2+}, and Mg^{2+}. When sodium balance and potassium balance exist, as under normal conditions, approximately 67% of filtered Na^+ and K^+ are reabsorbed through the early and late proximal tubule (Costanzo 2006).

The loop of Henle follows the late proximal tubule and is unique in that only one section of its three participates in active transport. The thin descending limb is water-permeable but

ion-impermeable, resulting in net reabsorption of water. The thin ascending limb is water-impermeable, causing a passive reabsorption of Na^+ to maintain osmotic balance. Only the cells of the thick ascending limb contain an active transporter, the $Na^+/K^+/2Cl^-$ cotransporter, even though this section is also water-impermeable. Potassium diffuses from these cells back into both the lumen of the nephron and into the capillary. Passive paracellular reabsorption of cations such as Mg^{2+} and Ca^{2+} also occurs in this segment (Costanzo 2006).

The early distal tubule remains relatively water-impermeable and contains one cotransporter for Na/Cl. The late distal tubule consists of two cell types: the α-intercalated cell and the principle cell. The α-intercalated cell is primarily responsible for K^+ reabsorption, and contains a proton pump as well as a H^+/K^+ antiporter. The principle cell is primarily responsible for K^+ secretion via increased lumen membrane permeability to both K^+ and Na^+. These mechanisms are important in maintaining potassium balance in the presence of changes in dietary K^+ intake; potassium balance must be maintained to ensure proper functioning of excitable tissues such as nerves, cardiac muscle, and skeletal muscle (Costanzo 2006).

Filtration of proteins and dextrans, or glucose polymers, from the glomerulus into Bowman's capsule is dependent on molecular size. The glomerular capillary poses a number of size-limiting obstacles to filtration. The endothelial membrane of the capillary wall is the least limiting, containing pores approximately 70-100 nm large (Costanzo 2006). This size allows for the passive filtration of most solutes, including plasma proteins such as albumin, but not blood cells. However, the rest of the capillary wall - the three-layer basement membrane and the epithelial wall - prevent further filtration of plasma proteins and other similarly sized molecules. The epithelium contains filtration slits, which are smaller than the pores of the endothelium at only 25-60 nm diameter (Costanzo 2006). In addition to size, molecular charge also affects

filtration capability due to glycoproteins throughout the glomerular capillary wall. These glycoproteins carry a negative electrostatic charge, thus attracting positively charged molecules and repelling those with a negative charge. This "charge barrier" further inhibits filtration of plasma proteins that are negatively charged. Dextrans are variably affected by these barriers, as their size can vary greatly depending on the number of glucose subunits and the conjugate; most dextran preparations used in clinical applications are between 40,000 to 70,000 Da. In addition, a study published by Asgeirsson et al. (2007) reported that polysaccharides such as dextrans appear to be more permeable across the glomerular capillary due to their linearity; they are less hindered by pore size barriers than the globular protein. As discussed in the following section, glucans are also linear polysaccharides and likely conform to the same permeability as dextrans.

Chemistry of (1→3)-β-D-Glucans

Glucans are carbohydrate polymers that are a component of the cell wall in various pathogenic and saprophytic fungi such as *Aspergillus* species, *Candida albicans*, *Saccharomyces cerevisiae*, and the shiitake mushroom *Lentinula edodes*. These polysaccharides are composed of multiple D-glucose subunits connected by 1,3 linkages; many glucans also have side chain branches linked at the 1,6 position. In 2001, Douglas reported on the synthesis of fungal (1→3)-β-glucans catalyzed by the plasma membrane enzyme UDP-glucose (1→3)-β-D-glucan β(3)-D-glucosyltransferase. Essentially, within the fungal organism, the enzyme reacts with UDP-glucose as its intracellular substrate, producing linear β1,3-glucan chains that are released into the cell wall space and connected to chitin, via β1,4 linkages, to form the cell wall. During fungal infection, such as candidiasis or aspergillosis, these glucans are released into the patient's systemic circulation (Miyazaki et al. 1995; Obayashi et al. 1995, 2008) and can be detected by

serum testing. The most common assay, the G-test, employs *Limulus*, a (1→3)-β-D-glucan and lipopolysaccharide (LPS)-specific lysate from amebocytes of the horseshoe crab. In 2008, Obayashi published data from autopsy cases that supported the use of clinical glucan serum tests in the diagnosis of mycotic infection; these assays for (1→3)-β-D-glucans have been tested and used clinically for several years. However, Digby et al. (2003) had observed five years previously that this assay was not specific to fungal infection; in their studies, ICU patients with bacterial infections or polymicrobial infections also tested positive for serum (1→3)-β-D-glucans. Interestingly, as a result of their 1995 study, Miyazaki et al. theorized that the release of β-glucans by the fungal organism may be a mechanism used to escape recognition by the host immune system. They hypothesized that the polysaccharides might block phagocytic receptors for β-glucans. It is now known that glucans have a wide variety of effects on the host immune system, which are described in greater detail below.

Glucans differ in their number of glucose subunits, degree of side chain branching, molecular mass, solution conformation, and polymer charge (Kulicke et al. 1997; Mueller et al. 2000). These variations influence the activity and receptor-ligand interactions of each glucan.

As described in Table 1, glucan phosphate is a mid-weight polysaccharide (157,000 Da) with no side chain branching (Fig. 1). It has been employed extensively *in vitro* by our laboratory and several others in the study of glucan pharmacokinetics and biological activity. Laminarin is a small glucose polymer (7700 Da) with a side chain branching frequency of approximately 1:10 (Fig. 2). Unlike glucan phosphate and scleroglucan, laminarin does not appear to have biological or immunological effects *in vivo*. Both laminarin and glucan phosphate have a single helical solution conformation, as seen in Figure 3. Scleroglucan is a polysaccharide with a large molecular mass of approximately 1,000,000 Da, higher than any

other synthetic glucan molecule employed by our laboratory. It also has a high frequency of side chain branching, averaging 1:3. Scleroglucan differs from glucan phosphate and laminarin in that it exists in solution as a triple helix (Fig. 4 and 5).

Table 1: Characteristics of three experimental glucans. Adapted from Mueller et al. (2000) The influence of glucan polymer structure and solution conformation on binding to (1→3)-β-D-glucan receptors in a human monocyte-like cell line. *Glycobiology* **10:**339-346. and Rice et al. (2002) Human monocyte scavenger receptors are pattern recognition receptors for (1→3)-β-D-glucans. *J Leukoc Biol.* **72:**140-146.

Polysaccharide	**Molecular mass**	**Degree of side chain branching**	**Type of glycosidic linkage**
Glucan phosphate	157,000 Da	None	β-(1→3)
Laminarin	7,700 Da	1:10	β-(1→3), (1→6) side chains
Scleroglucan	~1,000,000 Da	1:3	β-(1→3), (1→6) side chains

Polysaccharide	**Polymer charge**	**Solution conformation**
Glucan phosphate	Weak polyanion	Single helix
Laminarin	Neutral	Single helix
Scleroglucan	Weak polyanion	Triple helix

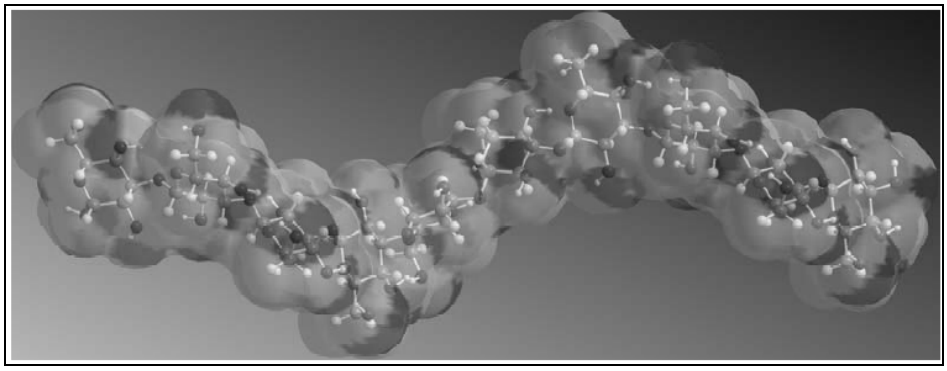

Figure 1: Chemical structure of a 1→3-β linked glucose polymer with low level of side chain branching, similar to glucan phosphate. Source: Adams et al. (2008) Differential high affinity interaction of dectin-1 with natural or synthetic glucans is dependent upon primary structure and is influenced by polymer chain length and side chain branching. *J Pharmacol Exp Ther.* **325:**115-23: used by permission.

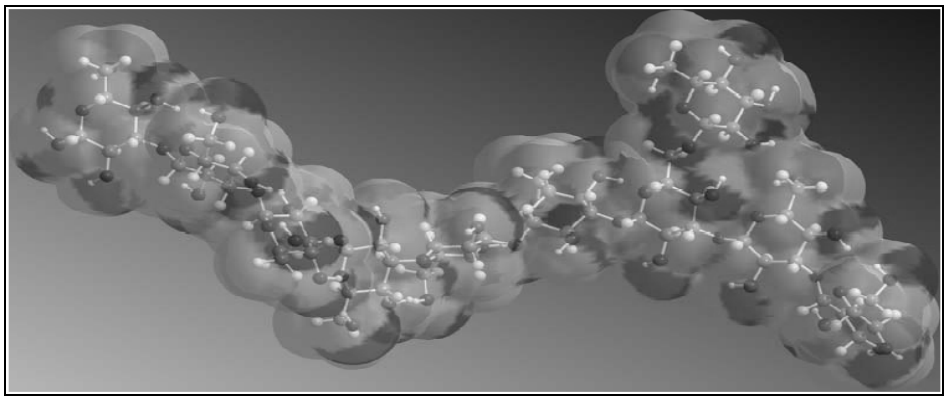

Figure 2: Chemical structure of a 1→3-β linked glucose polymer with side chain branching at various positions, similar to laminarin. Source: Adams et al. (2008) Differential high affinity interaction of dectin-1 with natural or synthetic glucans is dependent upon primary structure and is influenced by polymer chain length and side chain branching. *J Pharmacol Exp Ther.* **325:**115-23: used by permission.

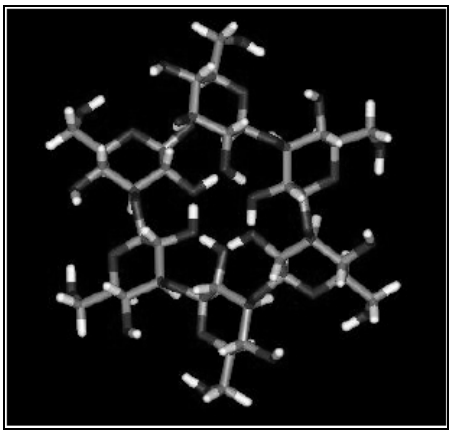

Figure 3: End view of a single helical glucan structure. When in solution, glucan phosphate and laminarin exist predominantly as single helices. Source: Williams et al. (2003) Recognition of fungal glucans by pattern recognition receptors. *Recent Devel Carbohydrate Res.* **1:**49-66: used by permission.

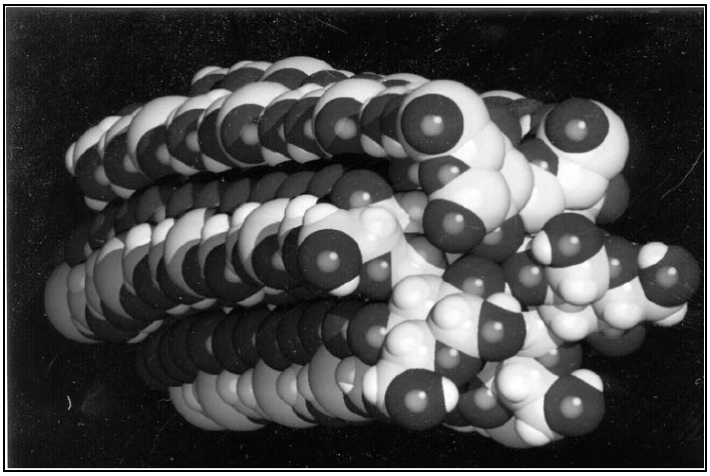

Figure 4: Chemical structure of a triple helical glucan polymer: three individual glucan polymer strands held together by hydrogen bonds at the C-2 hydroxyl at the center of the backbone chain, similar to scleroglucan. Used by permission from Williams (8 December 2008).

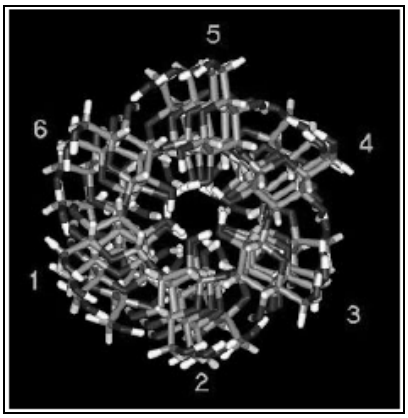

Figure 5: End view of triple helical glucan structure, similar to scleroglucan. Side chain branching is characteristic of scleroglucan but is not seen in this representation. Source: Williams et al. (2003) Recognition of fungal glucans by pattern recognition receptors. *Recent Devel Carbohydrate Res.* **1:**49-66: used by permission.

In the last several years, the characterization of the chemical structures of various glucans has been augmented with the development of a nuclear magnetic resonance (NMR) spectroscopy assay specific for (1→3)-β-D-glucans by Lowman et al. (2001, 2003). NMR spectroscopy allows for the identification and verification of chemical structures of proteins without affecting or destroying the sample. This procedure analyzes the resonance frequency of nuclei in the molecule and converts those frequencies into chemical shift values, which can then be compared to a reference chemical shift, usually tetramethylsilane (Reusch 1991). The glucan-specific NMR assay developed by Lowman and Williams in 2001 is based on the standard protein NMR analysis and provides a reliable, solvent-free method for identifying, characterizing, and quantitating the glucan dry-weight content within a matrix, such as extracts from a microbial or plant cell wall, without influencing any of their chemical or biological characteristics. Their assay reduced the time needed to perform this analysis; previous methods of analyzing glucan content of a complex matrix required 1-2 days, whereas the NMR assay requires a few hours.

Immunobiology of (1→3)-β-D-Glucans

Glucans are pathogen-associated molecular patterns or PAMPs. PAMPs are defined as molecules or motifs shared by a related group of microorganisms but not associated with human or host cells. PAMPs interact with pattern recognition receptors (PRRs) within the innate immune system and cause numerous organism-dependent biological effects. Common PAMPs include lipopolysaccharide A (LPS) and peptidoglycan; toll-like receptors are common PRRs. As pathogen-associated molecular patterns, glucans are known to interact with several cellular receptors throughout the body. In 1985, Czop and Austin identified the first β-glucan-specific receptor, a human monocyte receptor that influences the phagocytosis of activators of the alternative complement pathway. Since that time, numerous glucan pattern recognition receptors (PRRs) have been characterized, including the type 3 complement receptor (CR3; Ross et al. 1987; Thornton et al. 1996), scavenger receptors (Rice et al. 2002), and a C-type lectin-like receptor named Dectin-1 (Brown et al. 2001, 2002, 2003). These receptors have been found on cells of the innate immune system such as macrophages, neutrophils, natural killer (NK) cells, dendritic cells, and some T cell subtypes (Brown and Gordon 2003, Williams et al. 2003), but also on cells throughout the body, including epithelial cells (Ahren et al. 2001), vascular endothelial cells (Lowe et al. 2002), fibroblasts (Kougias et al. 2001), and anterior pituitary cells (Breuel et al. 2004). The observation of these receptors on non-immune cells indicates that glucans, in addition to causing indirect systemic responses through their interactions with immune system elements, may also directly affect the function of cells throughout the body (Kougias et al. 2001).

Glucans are biologically unique molecules. They have been identified as a potential target for antifungal pharmacological intervention; echinocandin drugs targeting (1→3)-β-D-

glucans inhibit their synthesis, thus inhibiting cell wall formation and fungal growth (Onishi et al. 2001). They have also been identified as potential pharmacologic substances themselves. Several researchers have investigated the numerous immunobiologic effects of β-glucans including anti-inflammatory and anti-cancer effects as described below.

Glucans are known to stimulate and modulate the innate immune response through their interactions with various receptors. For example, Dectin-1 has been identified as a major glucan receptor on macrophages, neutrophils, and dendritic cells; its interaction with glucans mediates phagocytosis of these polysaccharides (Herre et al. 2004). This receptor is also responsible for the production of TNF-α during the inflammation response to yeasts and zymosan, another β-glucan (Brown et al. 2003). The glucan-receptor interaction effect is not limited to cells of the immune system, however. In 2001, Kougias et al. published the first evidence for the presence of glucan-specific receptors and glucan binding sites on non-immune cells, in this case normal human dermal fibroblasts (NHDF). They discovered that glucans not only bind to specific sites on NHDF, they also enhance the activity of NF-κB and the genetic expression of proinflammatory cytokines through their interaction with these receptors. This observation signifies that the body's response to glucans may not be solely dependent upon cells of the immune system (Kougias et al. 2001).

β-Glucans have also been identified as anti-tumor polysaccharides. Hong et al. (2004) described the enhancement of the antitumor monoclonal antibody (mAb) effect by both yeast (1→3,1→6)-β-glucans and barley (1→3,1→4)-β-glucans. When either glucan was administered orally, using a murine tumor model, the glucan was internalized by macrophages, degraded in the bone marrow, and taken up into granulocytes via CR3. In contrast, intravenously-administered (1→3)-β-glucans are taken up directly from the circulation by CR3 on

granulocytes, as previously reported by Hong et al. (2003). The presence of glucans within the granulocytes enhanced their ability to kill tumor cells coated with inactivated C3b (iC3b; deposited by natural antitumor antibodies). This response, however, required the presence of CR3 on granulocytes and iC3b on tumor cells; if either was absent, tumor regression mediated by β-glucans and mAb did not occur. Additional studies have found that β-glucans have a cytotoxicity-priming effect on cells other than granulocytes, including neutrophils and NK cells (Vetvicka et al. 1996).

Pharmacokinetics of (1→3)-β-D-Glucans

Our laboratory has investigated and characterized many of the pharmacokinetic properties of (1→3)-β-D-glucans following both intravenous and oral administration. In 2004, Rice et al. investigated the pharmacokinetics of β-1,3-glucans after intravenous administration in a murine model. They found that glucan phosphate demonstrated a longer half-life for elimination from plasma, a lower volume of distribution, and a lower plasma clearance rate than either scleroglucan or laminarin. Their results indicate the possibility that some properties of glucans, i.e. molecular weight, solution conformation, or degree of branching, may influence their pharmacokinetic properties. Select characteristics from this study are found in Table 2.

Table 2. Pharmacokinetic characteristics for plasma laminarin, glucan phosphate and scleroglucan following intravenous administration. Adapted from Rice et al. (2004) Pharmacokinetics of fungal (1-3)-beta-D-glucans following intravenous administration in rats. *Int Immunopharmacol.* **4:**1209-15.

Parameter	Laminarin	Glucan phosphate	Scleroglucan
Distribution half-life, min	3.7 ± 1.3	4.3 ± 0.7	2.1 ± 0.5
V_D elimination, mL/kg	540 ± 146	350 ± 88*	612 ± 154
Half-life elimination, h	2.6 ± 0.2	3.8 ± 0.8[§]	3.1 ± 0.6
Clearance, total, mL/kg/h	102.6 ± 17.4	41.9 ± 5.8*,[§]	116.7 ± 18.9
Area under the curve (AUC), mcg/mL/hr	10.6 ± 1.2	26.0 ± 3.4	9.5 ± 0.8

Laminarin and scleroglucan were administered 1 mg/kg; glucan phosphate was administered 3.125 mg/kg.
*Significantly different from scleroglucan.
[§]Significantly different from laminarin.

Rice et al. (2005) also published the absorption and clearance of glucan phosphate, scleroglucan, and laminarin following oral administration in a murine model. Several pharmacokinetic characteristics were elucidated in this study: maximum concentration peaks, clearance parameters, and biological effects including intestinal binding and increased survival rates in the presence of challenge with *Staphylococcus aureus* or *Candida albicans*. Selected values are represented in Table 3. In addition to these data, they reported glucan phosphate demonstrated peak concentrations in plasma at 4 hours following administration; laminarin demonstrated two peak concentrations at 3 hours and 12 hours following administration, as did scleroglucan at 15 min and 3 hours. After 24 hours, 27 ± 3% of the maximum glucan phosphate level and 20 ± 7% of the maximum laminarin level remained in plasma; scleroglucan was virtually cleared from plasma at 12 hours, with approximately 5% of the maximum level remaining. Rice et al. (2005) also observed that the expression of Dectin-1 (in gut-associated

lymphoid tissue, or GALT, cells) and TLR2 (in dendritic cells) increased after oral glucan administration.

Table 3. Bioavailability of orally administered glucans. Adapted from Rice et al. (2005) Oral delivery and gastrointestinal absorption of soluble glucans stimulate increased resistance to infectious challenge. *J Pharmacol Exp Ther*. **314:**1079-1086.

Parameter	**Laminarin**	**Glucan phosphate**	**Scleroglucan**
Area under the curve (AUC), mcg/mL/hr	0.521 ± 0.147	0.120 ± 0.038	0.381 ± 0.229
Bioavailability, %	4.9%	0.5%	4.0%
Maximum concentration (C_{max}), ng/mL	115 ± 33	41.5 ± 3.4	355 ± 281

While the absorption and distribution of (1→3)-β-D-glucans has been characterized following both intravenous and oral administration, the method of excretion has not been elucidated. Therefore, our studies were designed to test the hypothesis that intravenously- and orally-administered β-glucans are excreted by the kidneys but are metabolized into smaller polymers prior to renal processing to allow for filtration and secretion into the nephron and, therefore, excretion in urine.

CHAPTER 2

MATERIALS AND METHODS

Animals

Age- and weight-matched male Sprague-Dawley rats (Harlan Sprague-Dawley, Indianapolis, IN) were used. Ages varied from 7 weeks to 16 weeks and weights varied from 238 g to 456 g; however, both age and weight were matched within experimental groups. Animals were housed together in multiple cages, on a 12-hour light/dark cycle, with food and water available ad libitum. Rats were weighed and fasted 18 hours prior to each experiment. Study protocol was approved by the University Committee on Animal Care, East Tennessee State University, Johnson City, Tennessee.

Glucans

(1→3)-β-D-Glucan phosphate was prepared and chemically characterized as previously described by Williams et al. (1991), Ensley et al. (1994), and Kim et al. (2000). Scleroglucan, a β-(1→3),(1→6)-glucan, was prepared and chemically characterized as previously described (Pretus et al., 1991). Laminarin, a β-(1→3),(1→6)-glucan, was purchased from Sigma-Aldrich (St. Louis, MO) and was chemically characterized as previously described (Mueller et al. 2000). The polymers were screened for endotoxin contamination with the Endospecy assay (Seikagaku/Cape Cod Associates, Falmouth, MA) according to manufacturer's instructions. Endotoxin levels were ≤0.3 IU/mg.

Preparation of Fluorescently Labeled Glucans

A diaminopropane (DAP) moiety was added to the reducing terminus of the glucan by the method of Kougias et al. (2001). Briefly, the DAP was attached to the reducing terminus of

the carbohydrate polymer by sodium borohydride reduction. The reaction mixture was dialyzed against 18-MΩ ultrapure pyrogen-free water and lyophilized to dryness. The glucan was stored at –20°C. Aliquots of the DAP-glucan derivatives were analyzed by gel permeation chromatography/multi-angle laser light scattering (GPC/MALLS), 1H NMR, and 13C NMR to confirm that the molecular weight, polydispersity, primary structure, and solution conformation were not altered by the derivatization. The carbohydrates were labeled with one of three AlexaFluor succinimidyl esters: 488, 555 or 647 (Molecular Probes, Eugene, OR). Briefly, the amine reactive AlexaFluor succinimidyl ester (Pierce Chemical, Rockford, IL) was attached to the DAP moiety located at the reducing terminus. Specifically, DAP-glucan (3 mg) was dissolved into sodium borate buffer (0.1 M, pH 8.5) at a concentration of 10 µg/µl in a total volume of 300 µl. In the case of particulate glucan, the insoluble DAP glucan was suspended in borate buffer, and the suspension was maintained by gentle agitation. AlexaFluor 488, 555 or 647 dye (5 mg) was dissolved in 35 µl of dimethyl sulfoxide. The dye solution was added to the DAP-glucan and incubated for 1 h in the dark, followed by addition of 300 µl of sodium borate buffer. The mixture was incubated overnight at ambient temperature on a reciprocating shaker at slow speed. The samples were incubated in foil-covered microfuge tubes to prevent exposure to light. The excess dye was removed by dialyzing (1000 Da molecular weight cutoff) against PBS overnight at room temperature. The advantage to this approach is that a single DAP and a single fluorescent moiety are attached to the reducing terminus of the polymer without changing the basic physicochemical characteristics of the carbohydrate ligand. Addition of the DAP and fluorescent tag does not alter binding of the glucan polymer to recombinant Dectin (data not shown). The labeling efficiency (>90%) was determined by flow cytometric analysis using recombinant Dectin-1.

Surgical Implantation of Microdialysis Catheter

All surgical instruments were sterilized in an autoclave (132 °C and 30 PSI for 15 minutes) prior to surgery. Sterile guide cannulae and probes were obtained from Bioanalytical Systems (MD-2212 and MBR-5, West Lafayette, IN). Each rat was given an intraperitoneal injection of ketoprofen (1.0 mg/mL) 15 minutes prior to a 1:1 ratio of ketamine (100 mg/mL) and xylazine (20 mg/mL) injected intraperitoneally. All injections were given in the volume of 1% of body weight. Once under anesthesia, the incision area was shaved and sterilized topically with alcohol. The animal was then laid on a heating pad to maintain body temperature and placed into a stereotaxic instrument with its nose placed into a Kopf mask. A mixture of isoflurane and oxygen was administered through the mask for the duration of the surgery to provide additional anesthesia and to aid in regular respiration. A midline incision was made in the scalp using a sterile scalpel to expose the midline suture and the bregma landmark. One complete intrusion was drilled into the skull using a Dremel Moto-Tool (Robert Bosch Tool Corporation, Racine, Washington) with a 1/32" bit at the coordinates 0.3 mm lateral and 1.5 mm caudal to bregma. Two partial intrusions were also drilled approximately 1 mm from the complete intrusion. Two skull screws were placed into the partial intrusions and anchored using ethyl cyanoacrylate to help anchor the acrylic cap used to hold the guide cannula in place. The guide cannula was then lowered into the complete intrusion and dental acrylic was applied surrounding the cannula and the two screws and allowed to dry. Once the acrylic was dry, the incision was closed with sutures. The animal was then given 10 cc of sterile Ringer's lactate subcutaneously (SQ) for rehydration purposes and placed on the heating pad into a paper-towel-lined cage until recovery from anesthesia was complete. Once awake and alert, the animal was placed back into a bedding-lined cage with unlimited access to food and water. Animals were

monitored following surgery for post-operative complications. Three rats expired during the procedure; the other five survived and healed with no complications.

Preparation of Artifical Cerebrospinal Fluid

Sterile artificial cerebrospinal fluid (CSF) was prepared as described by Moghaddam et al. (1989). Briefly, several 10X stocks were prepared in sterile 50 mL conical tubes, using 18 MΩ deionized water. These solutions were:

#1: 1450 mM NaCl (8.47g/100mL)

#2: 27 mM KCl (0.201g/100mL)

#3: 10 mM MgCl2●6H2O (0.203g/100mL)

#4: 20 mM Na2HPO4 (0.248g/100mL), pH 7.4

#5: 12 mM CaCl2●2H20 (0.176g/100mL)

On the day of use, 1.00 mL of each stock was combined in the order given and diluted to 10 mL with 18 MΩ deionized water, mixed thoroughly, and filtered through a sterile 0.22µ filter into a sterile 50 mL conical tube.

Experimental Protocol for Laminarin Microdialysis

The surviving rats were given a 14-day recovery period following surgery. On the day of microdialysis, the rats were sedated with isoflurane, then maintained on a combination of isoflurane and oxygen administered through a nose mask for the duration of the procedure, which provided constant anesthesia as well as assisting with regular respiration. The animals were kept on a warm-water bed throughout the procedure to maintain proper body temperature. When the animal was under anesthesia, as determined by slow rhythmic breathing and lack of response to hindpaw pinching, an area approximately 4 cm in diameter at the lateral base of the neck was shaved and cleaned with 95% ethanol. An incision was made to expose the right

jugular vein, and an intravenous line was established. Placement of the line was verified by drawing back blood with the syringe before injecting approximately 1 cc of sterile Ringer's lactate to flush the line. A midline abdominal incision was also made in the latter two rats to allow access to the urinary bladder for urine collection. The microdialysis probe was inserted into the cranial guide cannula; infusion of sterile artificial CSF was begun at 2 μg/min (in the third rat, infusion was increased to 2.5 μg/min after 90 minutes). After 30 minutes of CSF infusion, the distal 2 mm of the animal's tail was removed, and a tail blood sample was collected using a SAFE-T-FILL125 μL EDTA mini capillary tube (Ram Scientific, Yonkers, NY). A loading dose of fluorescently-labeled laminarin, 1 mg/kg, was given via the intravenous line. Infusion of laminarin, 0.25 mg/kg/hr, was begun immediately following the loading dose. The laminarin was infused for 5 hours; CSF samples were collected over 30-minute increments and blood samples were obtained every 30 minutes. In the latter two rats, urine was also drawn from the urinary bladder using a needle and syringe. Throughout the procedure, rats were closely monitored to assess level of sedation. When the laminarin infusion was completed, CSF infusion was also stopped. Rats were then euthanized by exsanguination. In the fourth rat, 75 μg methylene blue was introduced into the guide cannula to mark its placement. Two lateral cranial incisions were made through each animal's skull cap, the cannula and acrylic cap were removed from each brain, and the brains were harvested and stored in 10% buffered formalin phosphate (Fisher Scientific, Pittsburgh, PA).

Experimental Protocol for Surgical Injection of Glucan Phosphate

On the day of the procedure, the rats were sedated with isoflurane (Baxter, Deerfield, IL), then maintained on a combination of isoflurane and oxygen administered through a nose mask for the duration of the procedure, which provided constant anesthesia as well as assisting with

regular respiration. The animals were kept on a warm-water bed throughout the procedure to maintain proper body temperature. When the animal was under anesthesia, as determined by slow rhythmic breathing and lack of response to hindpaw pinching, sterile 5% dextrose (D5) solution was given SQ to aid in maintaining hydration and urine production. Two areas of the animal's skin were shaved: one approximately 4 cm in diameter at the lateral base of the neck, and the other approximately 3 cm in diameter on the abdominal midline. On the abdomen, a midline incision was made to expose the urinary bladder for urine collection. At the base of the neck, an incision was made to expose the left jugular vein, and an intravenous line was established. The distal 2 mm of the animal's tail was removed to allow for blood sampling. Control urine and tail blood samples were obtained. Fluorescently-labeled glucan phosphate, 1 mg/kg using a solution of 1 mg/mL in phosphate buffered saline (PBS), was injected directly into the left jugular vein. After injection, tail blood samples were collected in SAFE-T-FILL 125 µL EDTA mini capillary tubes every 15 minutes during hour 1, every 30 minutes during hour 2, and every 60 minutes following hour 2 through hour 6. Urine samples were collected every hour during the 6 hours. Hydration was maintained through tap water administered via oral gavage and through SQ injections of D5. Throughout the procedure, rats were closely monitored to assess level of sedation. After 6 hours, the experiment was terminated and animals were euthanized by exsanguination.

Experimental Protocol for Intravenous Injection of Glucans

The distal 2 mm was removed from each animal's tail to allow for blood sample collection. Control tail blood samples were drawn from each rat using 125 µL SAFE-T-FILL EDTA mini capillary tubes. Rats were temporarily anesthetized with isoflurane; the fluorescently-labeled glucans, at a dose of 1 mg/kg using a solution of 1 mg/mL in PBS, were

administered intravenously in the retro-orbital space. Rats were immediately placed into individual metabolic cages with water available ad libitum. Tail blood was drawn at 0.25, 0.5, 0.75, 1, 1.5, 2, 3, 4, 5, and 6 hours following dose. Urine was collected throughout the experiment via the metabolic cage. At 6 hours, rats were placed back into their original cages and fed.

Experimental Protocol for Oral Administration of Glucans

The distal 2 mm of each animal's tail was removed, and control tail blood samples were collected from each rat using 125 μL SAFE-T-FILL EDTA mini capillary tubes. The fluorescently-labeled glucans, at a dose of 0.95 mg/kg using a solution of 0.95 mg/mL in water, were administered using an oral gavage technique. Rats were immediately placed into individual metabolic cages with water available ad libitum. Tail blood was collected at 0.25, 0.5, 0.75, 1, 1.5, 2, 3, 4, 5, and 6 hours following dose. Urine was collected throughout the experiment via the metabolic cage. At 6 hours, rats were euthanized with carbon dioxide. Blood was drawn from the vena cava into EDTA-treated Vacutainer tubes and centrifuged; plasma was removed and frozen for later analysis. Kidneys and a section of jejunum (approx. 4 cm) were removed and placed in 4% paraformaldehyde for later histological analysis.

Experimental Protocol for Co-Administration of Glucan Phosphate and Lipopolysaccharide A

Rats were administered ultra-pure lipopolysaccharide A (LPS) from *Escherichia coli* 0111:B4 (List Biological Laboratories, Inc., Campbell, CA), 1 mg/kg intraperitoneally (IP), and allowed to rest for 1 hour. After 1 hour, fluorescently-labeled glucan phosphate was given orally at a dose of 0.95 mg/kg, using a 0.95 mg/mL solution in water. The distal 2 mm of each animal's tail was removed, and tail blood samples were collected in 125 μL SAFE-T-FILL EDTA mini capillary tubes at 0.25, 0.5, 0.75, 1, 1.5, 2, 3, 4, 5, and 6 hours following dose. At 6

hours, rats were euthanized with carbon dioxide. Urine was drawn from the bladders with a sterile needle and syringe; urine was unobtainable from the remaining three rats. Blood was drawn from the vena cava into 4.0 mL EDTA BD Vacutainer tubes (Becton, Dickenson and Company, Franklin Lakes, NJ) and centrifuged at 2000 rpm using a Sorvall Legend RT benchtop centrifuge (Thermo Scientific, Waltham, MA); plasma layer was removed and frozen for later analysis.

Comparison of Administration Methods and Co-Administration of LPS

Three animals were employed for the experiment. One rat was administered ultra-pure lipopolysaccharide A (LPS), 1 mg/kg IP, and allowed to rest for 1 hour. After an hour, the LPS-dosed animal, as well as one other animal, were administered fluorescently-labeled glucan phosphate orally at a dose of 1 mg/kg, using a 1 mg/mL solution in water. The distal 2 mm of the tail was removed from the remaining animal and a control blood sample was obtained in a heparinized micro-hematocrit capillary tube. This animal was anesthetized with isoflurane and administered glucan phosphate at a dose of 1 mg/kg IV retro-orbitally, using a 1 mg/mL solution in PBS. Tail blood was drawn from the orally-dosed animal at 5, 10, 15, 20, 30, 45, 60, 90, and 120 minutes following dose, collected in heparinized micro-hematocrit capillary tubes (Fisher Scientific, Pittsburgh, PA). Blood samples were immediately centrifuged and plasma layer separated into a microcentrifuge tube. After 2 hours, rats were anesthetized with carbon dioxide. Blood was drawn from the posterior vena cava into EDTA BD Vacutainer tubes and centrifuged; plasma was removed and frozen for later analysis. Urine was drawn from the bladder and stored in microcentrifuge tubes. Kidneys were removed from the orally-dosed animal, and a section of jejunum was removed from the intravenously-dosed animals; the tissues were placed in 4% paraformaldehyde for histological analysis. Rats were then euthanized with carbon dioxide.

Detection of Fluorescent Glucans in Whole Tissues

Two animals were administered fluorescently-labeled oral glucan phosphate at a dose of 1 mg/kg using a 1 mg/mL solution in water. Two hours post-administration, animals were euthanized with carbon dioxide. Kidneys were removed... Kidney sections were submitted to the histology laboratory of the Department of Pathology (East Tennessee State University, Johnson City, TN) for embedding, sectioning, and staining or for frozen sectioning and staining. Various fixatives were employed, one per tissue sample: 100% methanol, 4% paraformaldehyde, HistoChoice fixative or periodate-lysine-paraformaldehyde (PLP) fixative; tissue for frozen section was fresh frozen using OCT compound. Sytox green was used as a counter-stain.

Detection of Fluorescent Glucans in Plasma and Urine

Blood samples were centrifuged at 2000 rpm for 10 minutes. Samples from plasma, CSF, and urine, as well as standards and controls, were pipetted into COSTAR black 96-well microplates (Corning Life Sciences, Lowell, MA) and analyzed on a SpectraMax Gemini XPS Plate Reader (Molecular Devices, Sunnyvale, CA) using SoftMax Pro software For the experiments using glucans labeled with AlexaFluor 647, the microplate reader parameters were set at an excitation of 645 nm and emission of 670 nm. For the experiments using glucans labeled with AlexaFluor 488, the excitation was 485 nm and the emission was 520 nm. For the experiments using glucans labeled with AlexaFluor 555, the excitation was 545 nm and the emission was 570 nm.

Chromatography

Each urine sample was subjected to size-exclusion chromatography for peak determination and fractionation. Briefly, a portion of each urine sample was injected into an ÄKTA purifier 10 (Amersham Biosciences, Piscataway, NJ) and passed through a desalting

column (molecular weight cutoff of 5000 Da). The sample was fractionated based on volume into a COSTAR black 96-well microplate, to separate free fluorescence from bound. The subsequent microplates were analyzed on a FLUOstar Galaxy Plate Reader with the appropriate parameters as described above.

Determination of Glucan Molecular Mass

From the chromatography microplates in one experiment, the samples representative of the higher molecular weight peak, or peak 1, were combined and lyophilized; the molecular mass was then determined by gas permeation chromatography/multi-angle laser light scattering (GPC/MALLS). In each case, the total volume of the fraction to be combined and lyophilized was 3.5 mL.

Verification of Glucan Structure Presence in Urine

On the day of the procedure, the animal was sedated with isoflurane then maintained on a combination of isoflurane and oxygen administered through a nose mask for the duration of the procedure, which provided constant anesthesia as well as assisting with regular respiration. The animal was kept on a warm-water bed throughout the procedure to maintain proper body temperature. When the animal was under anesthesia, as determined by slow rhythmic breathing and lack of response to hindpaw pinching, 0.5cc tap water was given by oral gavage. An area approximately 4 cm in diameter at the lateral base of the neck was shaved. An incision was made to expose the left jugular vein, and an intravenous line was established. A bolus injection of unlabeled glucan phosphate, 2 mg/kg, was given through the IV line. Immediately following the bolus, an infusion of glucan phosphate, 1 mg/kg/hr, was begun through the IV line. Sterile 5% dextrose solution (D5), 10cc, was administered SQ after beginning the infusion. Urine samples were collected periodically during the experiment and combined. Throughout the

procedure, rats were closely monitored to assess level of sedation. After 6 hours, the experiment was terminated, remaining urine was collected, and animal was euthanized by exsanguination. Control urine samples were obtained from age- and weight-matched Sprague-Dawley rats, unfasted. Urine was prepared for nuclear magnetic resonance spectroscopy (NMR) to confirm the presence of glucans in the urine. 500 µL from the experimental and control urine samples, as well as 500 µL control urine spiked with 2.5 mg/mL glucan phosphate, were pipetted into separate NMR tubes and submitted to Doug Lowman, PhD, Eastman Chemical Company for 1H-NMR spectroscopy and interpretation. Dr. Lowman's method was as follows:

> Briefly, proton NMR spectral data were collected using a JEOL Model Eclipse+ 600 NMR spectrometer operating at 80 ºC in 5-mm OD NMR tubes. For each sample, about 20 mg of isolate was dissolved in 1–mL of dimethyl sulfoxide-d6 (DMSO-d6) at 80 ºC. For the liquid urine samples, about 200 µL DMSO-d6 was combined with about 800 µL of liquid urine at room temperature. Proton chemical shifts were referenced to the residual DMSO-d6 proton resonance at 2.50 ppm. Generally, NMR spectral collection and processing parameters were the following: 25 ppm spectral width centered at 7.5 ppm, 32768 data points, 1024 scans, 15 sec relaxation delay, 2.18 sec acquisition time, and exponential apodization.

Remaining urine was lyophilized and stored. A portion of one urine sample was also submitted to the Department of Pathology at East Tennessee State University for urinalysis.

Data Analysis

Results from fluorescence spectroscopy and ÄKTA chromatography were evaluated using Excel 2003 (Microsoft Corporation, Redmond, WA) and Prism 5.01 (GraphPad Software, La Jolla, CA). Statistical analysis was performed using GraphPad statistical calculators. To

determine statistical significance between control and treated groups, a 95% confidence interval was calculated based on the mean and SEM. Significance was assumed when the treated group demonstrated a 95% confidence interval above, and not including, zero.

CHAPTER 3

RESULTS

Laminarin Microdialysis

Laminarin was initially chosen for the study of glucan transport across the blood-brain barrier due to its relatively small molecular weight (~7700 Da) compared to other glucans. Upon analysis of the samples obtained, no fluorescence was detected in any of the cerebrospinal fluid samples; however, fluorescence was detected in the plasma samples, indicating the presence of laminarin (data not shown). From these results, we concluded that laminarin was not transported across the blood-brain barrier into the cerebrospinal fluid but was still present in the vascular circulation. During the experiment with the third rat, we noticed that the urine had a greenish tint; we hypothesized that this could indicate the presence of laminarin in the urine, because the fluorescent 647 label on the laminarin gave the L647 solution a blue color. Because of this observation, we collected urine periodically throughout the experiment in addition to cerebrospinal fluid and plasma from the fourth and fifth animals; six urine samples were collected in total from the two animals. Upon fluorescence spectroscopy, a significantly high level of fluorescence was detected in the urine samples, suggesting the presence of laminarin in the urine (Fig. 6).

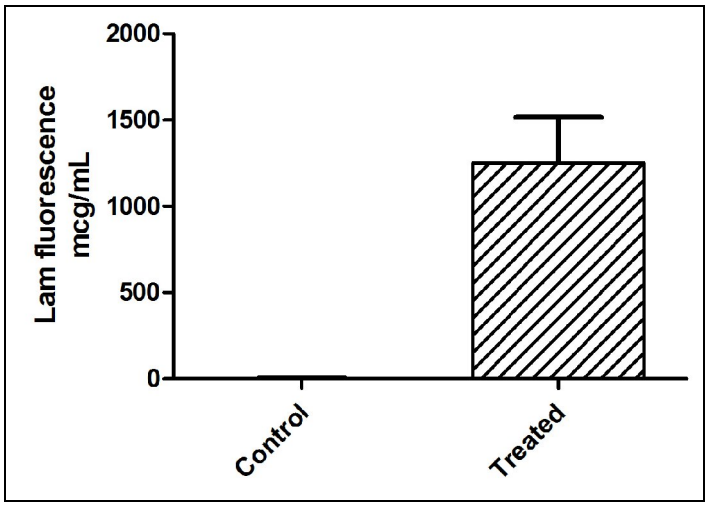

Figure 6. Laminarin (Lam) fluorescence is present in urine following intravenous infusion. Higher levels of fluorescence were observed in the samples from treated animals as compared to control animals. Data represented is mean ± SEM; 95% CI is 575 to 1931 mcg/mL; N=6.

Excretion of Intravenously-Administered Glucans

Glucan Phosphate

Following the results of the intravenous laminarin experiment, we wanted to investigate whether the observed glucan excretion was molecular-weight dependent. To test this hypothesis, we administered glucan phosphate intravenously; this polysaccharide has a higher molecular weight than laminarin (150,000 Da vs. 7700 Da). As seen in Figure 7, significance fluorescence was detected in the urine samples, suggesting the presence of glucan phosphate in the urine.

We subjected a portion of each urine sample to size exclusion chromatography using a desalting column with a molecular weight cutoff of 5000 Da. Given that the molecular weight of glucan phosphate is approximately 157,000 Da, and the molecular weight of the AlexaFluor label attached to the glucan is either 643 Da (for AlexaFluor 488) or 1250 Da (for AlexaFluor

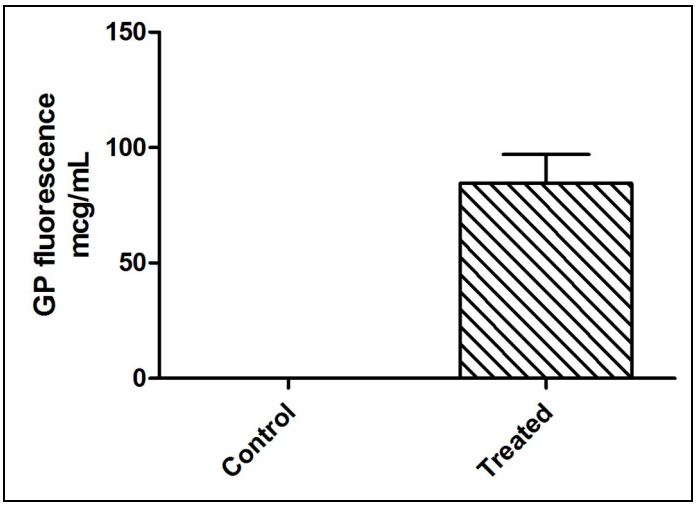

Figure 7. Glucan phosphate (GP) fluorescence is present in urine following intravenous injection. Higher levels of fluorescent glucan phosphate were observed in the samples from treated animals as compared to control animals. Data represented is mean ± SEM; 95% CI is 50 to 119 mcg/mL; N=5.

555 or 647), size exclusion chromatography provided an efficient means of separating the free fluorescent label from the fluorescent label still bound to the glucan molecules. In other words, the chromatography column was used to demonstrate whether the fluorescence observed in the urine samples originated from glucan molecules or from free fluorescent label that had been separated from the glucan and excreted on its own. Any molecules greater than 5000 Da came off the column in the first elution fraction of four mL; the remaining elution fractions contained molecules with molecular weights less than 5000 Da. Following analysis of these fractions by fluorescence spectroscopy, the results demonstrated that 66 ± 2% of fluorescence was observed in the first elution fraction, indicating that approximately 66% of the fluorescent molecules in the urine samples were larger than 5000 Da (Fig. 8).

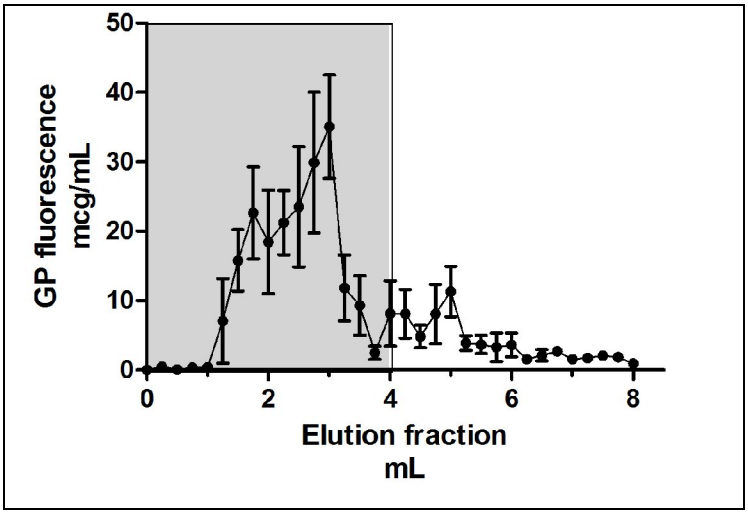

Figure 8. Chromatographic analysis of glucan phosphate (GP) fluorescence in urine following intravenous injection. The shaded peak denotes the first elution fraction containing molecules larger than 5000 Da; 66% of fluorescence was contained in this fraction. N=7.

To confirm that this fraction contained the injected glucan phosphate, we also analyzed a portion of each urine sample by gel permeation chromatography and multi-angle laser light scattering (GPC/MALLS), allowing for an approximation of the molecular weight of the molecules in solution. The light-scattering signal and refractive index detected by GPC/MALLS are shown in Figure 9. As seen in Table 4, GPC/MALLS confirmed that the majority of the molecules were of low molecular weight. These data, taken together, support glucan phosphate excretion in the urine following polysaccharide metabolism.

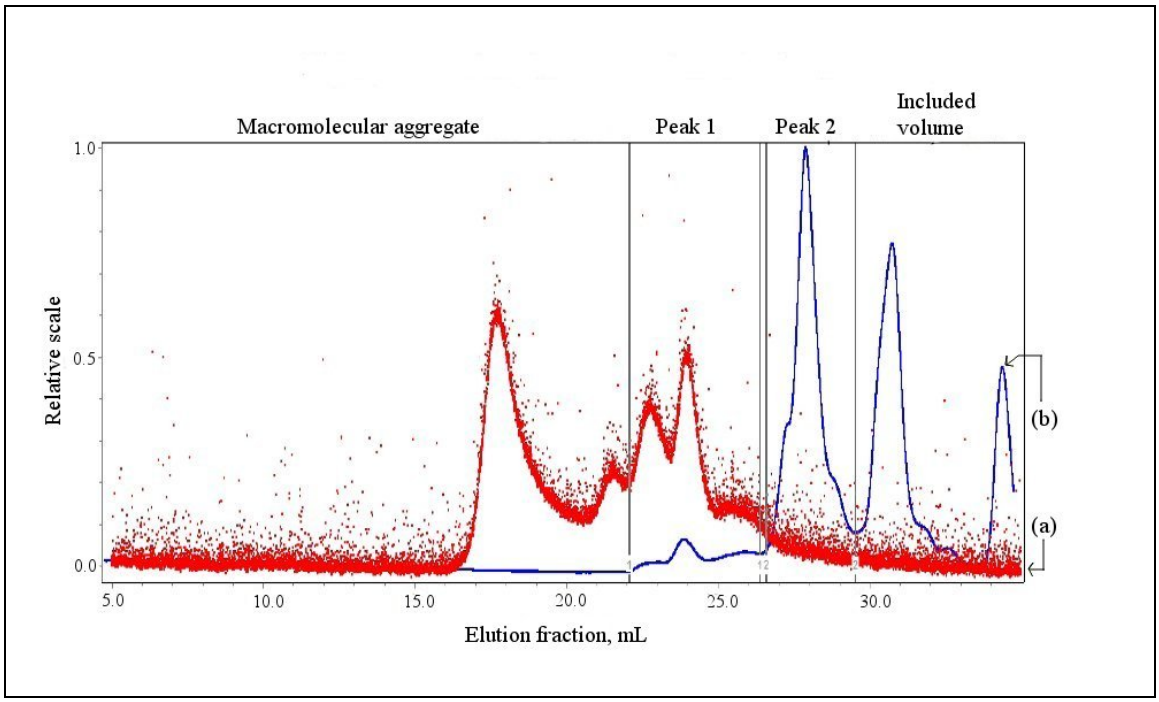

Figure 9. The majority of excreted glucans are of lower molecular weight than the original polymer. (a) denotes the light scattering signal; (b) denotes the refractive index. Peak 1 corresponds to a small amount of high molecular weight material, demonstrated by a relatively strong light scattering signal and low refractive index peak. Peak 2 corresponds to a larger amount of low molecular weight material, demonstrated by a relatively weak light scattering signal and elevated refractive index peak.

Table 4. Molecular weights of fluorescently-labeled glucan phosphate from urine as determined by GPC/MALLS. The molecular weight of the first peak roughly corresponds to the size of the injected glucan phosphate. The molecular weight of the second peak is significantly higher than the size of the fluorescent label, but significantly lower than the size of the glucan phosphate molecule.

Sample	MW (first peak), Da	MW (second peak), Da
1	144,000	38,600
2	162,000	2,860
3	189,000	6,870
4	189,000	3,710
Mean	**171,000**	**13,010**
SEM	**±11,022**	**±8,573**

Scleroglucan

At this point, we had evidence that small- and mid-weight glucans were excreted into the urine. The next step was to test our highest-weight glucan, scleroglucan, which has an average molecular mass of approximately 1,000,000 Da. As in the previous experiments, we injected the scleroglucan and collected urine samples for analysis (Fig. 10). These urine samples also demonstrated a noticeable peak within the first elution fraction (containing molecules >5000 Da) following ÄKTA chromatography (Fig. 11). This fraction represented 65 ± 11% of the total fluorescent molecules, indicating that approximately 65% of the fluorescence observed in the urine was from molecules larger than 5000 Da.

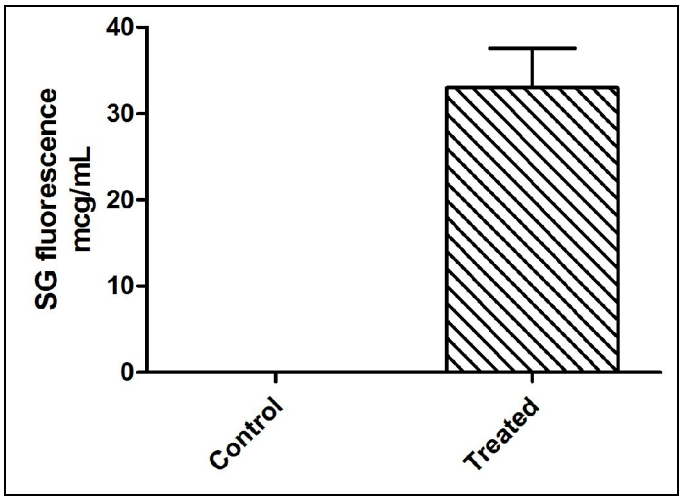

Figure 10. Scleroglucan (SG) fluorescence is present in urine following intravenous injection. Higher levels of fluorescent scleroglucan were observed in the samples from treated animals as compared to control animals. Data represented is mean ± SEM; 95% CI is 21 to 45 mcg/mL; N=6.

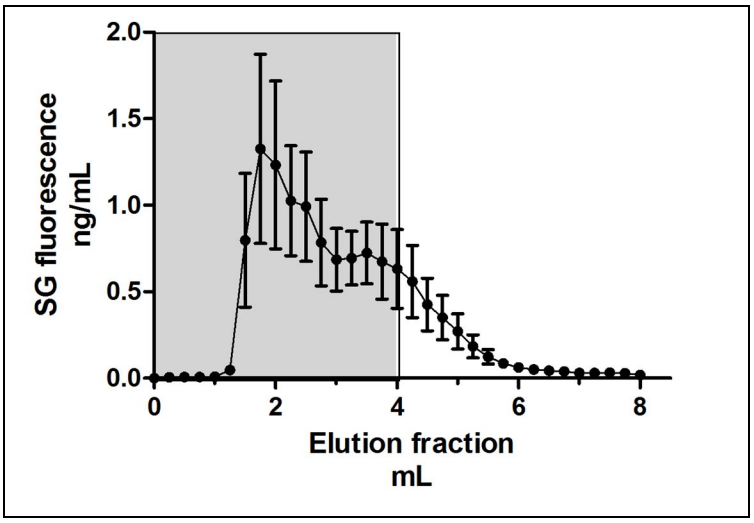

Figure 11. Chromatographic analysis of scleroglucan (SG) fluorescence in urine following intravenous administration. The shaded peak denotes the first elution fraction containing molecules larger than 5000 Da; 65% of fluorescence was contained in this fraction. N=6.

Laminarin

We now had data supporting glucan phosphate and scleroglucan excretion following intravenous administration, but we did not have data showing laminarin excretion following intravenous injection, only intravenous infusion. Because infusion methods administer a much higher total amount of glucan than injection, we opted to repeat the intravenous injection experimental protocol using laminarin. Results are similar to the injected glucan phosphate and scleroglucan experiments; significant fluorescence was detected in the urine samples (Fig. 12), while chromatography results indicated a clear peak in the first elution fraction (Fig. 13). This fraction contained 88 ± 1% of total fluorescence, demonstrating that 88% of the fluorescence in the urine could be attributed to molecules larger than 5000 Da.

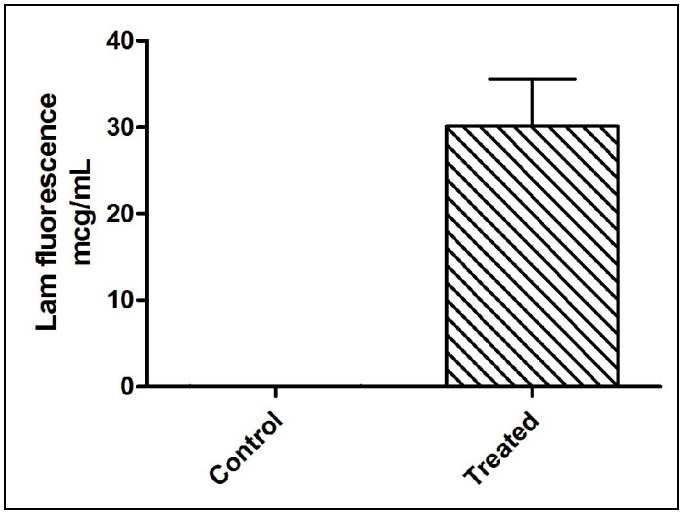

Figure 12. Laminarin (Lam) fluorescence is present in urine following intravenous injection. Higher levels of fluorescent laminarin were observed in the samples from treated animals as compared to control animals. Data represented is mean ± SEM; 95% CI is 16 to 44 mcg/mL. N=6.

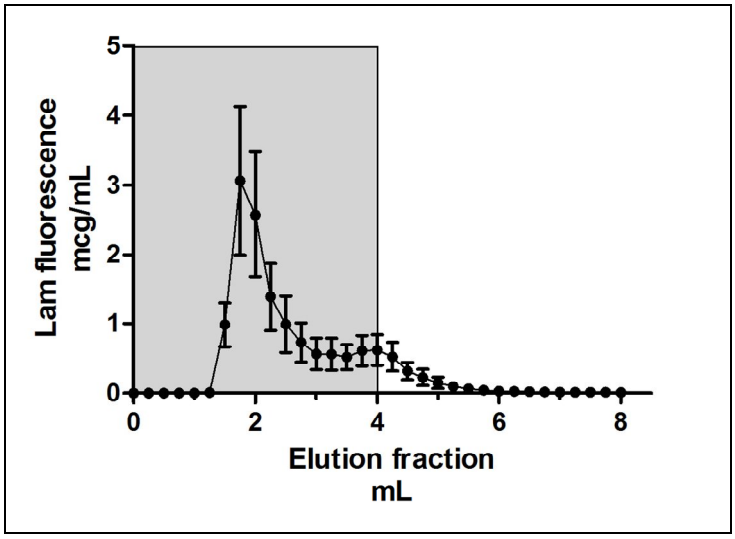

Figure 13. Chromatographic analysis of laminarin (Lam) fluorescence in urine following intravenous injection. The shaded peak denotes the first elution fraction containing molecules larger than 5000 Da. 88% of fluorescent molecules remained in this fraction; N=6.

Excretion of Orally Administered Glucan Phosphate

We had shown at this point that glucans are excreted by the kidneys following both intravenous infusion and injection without regard to molecular weight, because the

polysaccharides appear to be metabolized into smaller fragments prior to excretion. Our next step, therefore, was to look for glucan excretion following oral administration. Glucan phosphate was chosen as the polymer for this study; because excretion appears to be independent of molecular size, we opted to use the glucan polymer most widely characterized and employed in our other studies. Once again, our results indicated a significant level of fluorescence in the urine following oral administration (Fig. 14) with a clear first elution fraction peak demonstrated by size-exclusion chromatography (Fig. 15). This fraction contained 53 ± 6% of the total fluorescent molecules.

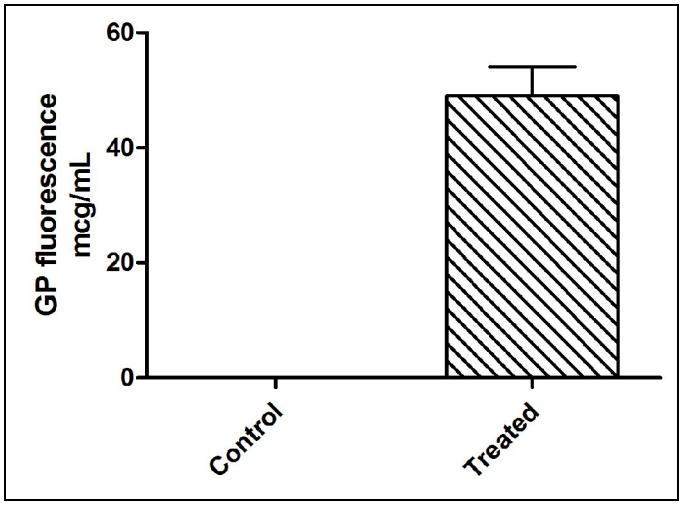

Figure 14. Glucan phosphate (GP) fluorescence is present in urine following oral administration. Higher levels of fluorescent glucan phosphate were observed in the samples from treated animals as compared to control animals. Data represented is mean ± SEM; 95% CI is 36 to 62 mcg/mL. N=6.

Table 5 summarizes the results of our experiments with intravenously- and orally-administered glucans. Infused laminarin, as expected, resulted in the highest urinary glucan levels due to the high amount of glucan received by the animal. Surgically injected glucan phosphate showed the next highest concentration of urinary glucan, followed by non-surgically

injected glucan phosphate and orally administered glucan phosphate. Injected laminarin and scleroglucan had the lowest concentrations of urinary glucan, but were still significantly higher than controls.

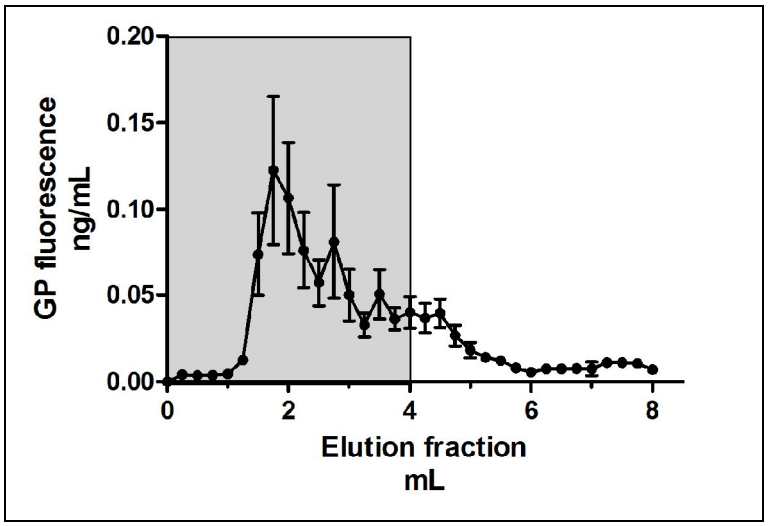

Figure 15. Chromatographic analysis of glucan phosphate (GP) fluorescence in urine following oral administration. The shaded peak denotes the first elution fraction containing molecules larger than 5000 Da; 53% of fluorescence remained in this fraction. N=4.

Table 5. Summary of concentrations of glucans in urine following administration.

Glucan	**Method of administration**	**Dose received (based on animal's weight)**	**Glucan concentration in urine, mcg/mL (mean ± SEM)**	**95% Confidence interval, mcg/mL**	**N (number of samples)**
Laminarin	IV infusion	300 to 362 µg	1253 ± 264	575 to 1931	6
Glucan phosphate	IV injection	396 to 422 µg	85 ± 13	50 to 119	5
Laminarin	IV injection	288 to 328 µg	30 ± 5	16 to 44	6
Scleroglucan	IV injection	238 to 248 µg	33 ± 5	21 to 45	6
Glucan phosphate	Oral gavage	396 to 456 µg	49 ± 5	36 to 62	6

Table 5 continued.

Glucan	Method of administration	Percent of fluorescent molecules in first elution fraction (>5000 Da), mean ± SEM	N (number of samples)
Glucan phosphate	Intravenous injection	66 ± 2%	7
Laminarin	Intravenous injection	88 ± 1%	6
Scleroglucan	Intravenous injection	65 ± 11%	6
Glucan phosphate	Oral gavage	53 ± 6%	6

Orally Administered Glucan Phosphate and Toxic Challenge

We had confirmed that glucans are excreted into the urine independent of molecular weight or administration method. The next experiment was designed to test whether the presence of a shock-like state, induced by intraperitoneal administration of lipopolysaccharide A, would affect gastrointestinal permeability to glucans, thus affecting absorption and excretion. LPS is an endotoxin contained in the outer membrane of gram-negative bacteria and, as such, triggers the innate immune system to secrete pro-inflammatory cytokines. The use of LPS is widely accepted as a method to model septic shock in experimental animals. In our experiments, upon administration of LPS to the animals, symptoms of illness were observed within 5 minutes and peaked within 60 minutes; these symptoms included lethargy, irritability and diarrhea. One unforeseen complication of using lipopolysaccharide A in the animals was a significantly decreased urine production due to dehydration and general malaise. Due to this, very small amounts of urine were collected from three of the six animals; the other three animals did not produce any obtainable urine. Nevertheless, two peaks are still clearly seen in the chromatography results, with a relatively strong first elution fraction (Fig. 16). 40 ± 2% of fluorescence was retained in this fraction.

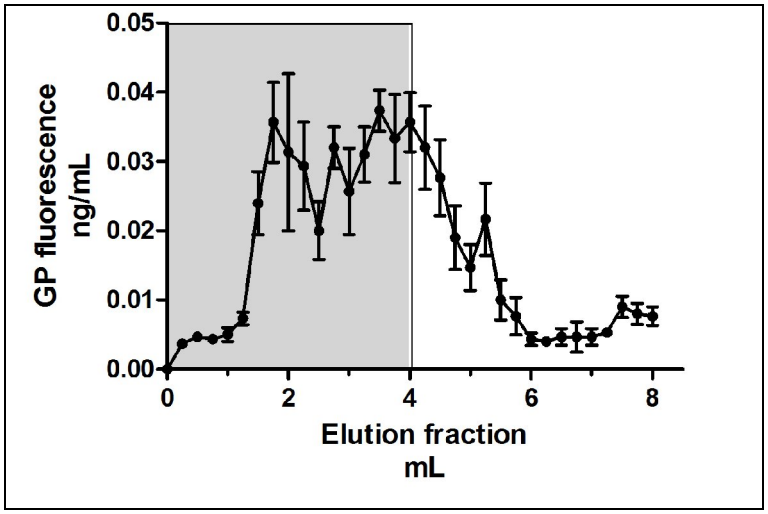

Figure 16. Chromatographic analysis of glucan phosphate (GP) fluorescence in urine following oral administration and LPS challenge. The shaded peak denotes the first elution fraction containing molecules larger than 5000 Da. This fraction contained 40% of total fluorescence; N=3.

Varying Administration Methods in the Presence or Absence of Toxic Challenge

The final experiment was designed to compare methods of glucan administration in the presence or absence of a shock-like state induced by LPS. One rat was administered oral glucan 1 hour post-LPS administration; the other two rats were not challenged with LPS but were administered glucans using different methods (intravenous versus oral). As seen in Figure 17, the animal that received intravenous glucan demonstrated the highest levels of urinary glucans, followed by the animal receiving oral glucan without challenge by LPS. The animal challenged with LPS demonstrated the lowest urinary glucan concentration; however, this result was still higher than control urine.

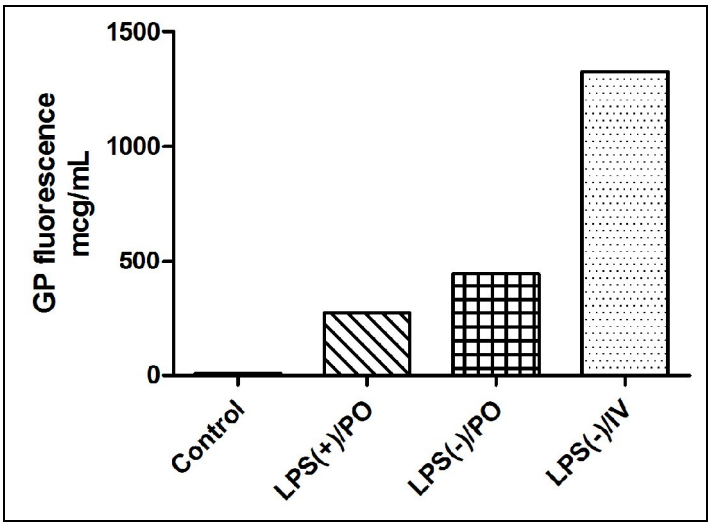

Figure 17. Comparison of glucan phosphate (GP) fluorescence in urine with different administration methods and LPS challenge. N=1 per group.
LPS(+)/PO: LPS-treated animal; oral glucan administration.
LPS(-)/PO: No LPS treatment; oral glucan administration.
LPS(-)/IV: No LPS treatment; intravenous glucan administration.

When these urine samples were subjected to size-exclusion chromatography, the sample from the animal administered with oral glucan demonstrated an evident peak within the first elution fraction, similar to the previous experiments, as seen in Figure 18. However, the samples from the orally-administered glucan animals, both in the presence and absence of LPS challenge, showed little to no peaks.

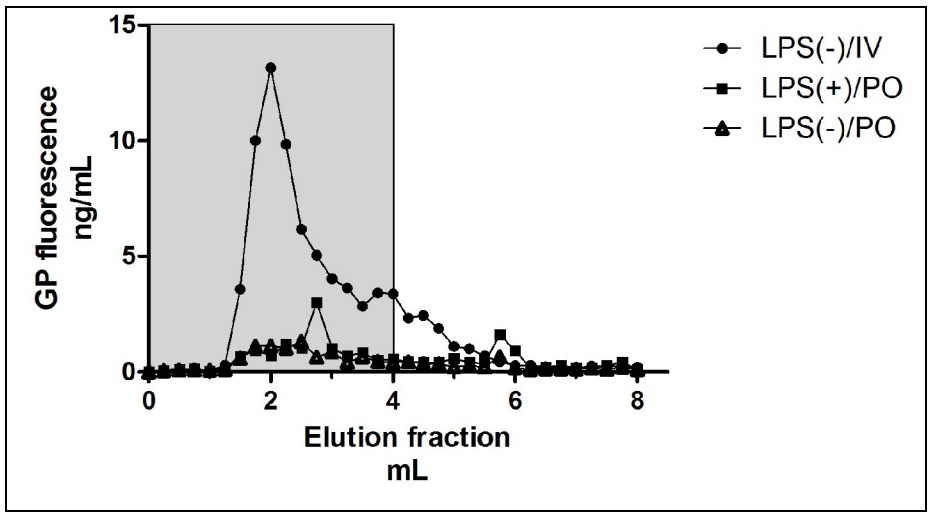

Figure 18. Chromatographic analysis of glucan phosphate (GP) fluorescence in urine with different administration methods and LPS challenge. The shaded peak denotes the first elution fraction containing molecules larger than 5000 Da.

Detection of Glucan Structure in Urine

To confirm the presence of glucan structure in the >5000 Da molecular fraction detected by our analyses with fluorescence spectroscopy, ÄKTA chromatography and GPC/MALLS, we prepared unlabeled glucan phosphate and administered it intravenously to one animal. A portion of the liquid urine sample was then subjected to nuclear magnetic resonance spectroscopy (NMR). Another portion of the sample was lyophilized and also submitted for NMR. Analysis and interpretation was provided by Dr. Doug Lowman. Figure 19 shows the results of the 1H-NMR analysis of the liquid urine samples. There are not proton NMR resonances in the pure glucan spectrum [Fig. 19 (d)] that also appear in the other three spectra [Fig. 19 (a), (b), and (c)]. Originally it was thought that the anomeric proton might be most diagnostic of the presence of glucan in the urine samples, but the anomeric proton does not appear clearly in any of the spectra from the urine samples, even the spiked sample. It was then hypothesized that the largest resonance in the glucan spectrum might be diagnostically useful, but on examination even the multiple resonance around 3.3 ppm does not appear in any of the urine samples.

Figure 20 depicts the NMR spectra from the lyophilized urine samples. From these spectra, is it clear that there is no evidence for glucan in the rat urine sample [Fig. 20 (b)]. Resonances at 4.53 ppm (not shown) and about 3.3 ppm in the reference glucan [Fig. 20 (c)] appear possibly to be present in the lyophilized rat urine sample. Because the doublet resonance from glucan near 3.73 ppm is not as evident in the urine sample, it is not possible to unequivocally indicate that the NMR spectrum demonstrates the presence of glucan in the lyophilized rat urine sample.

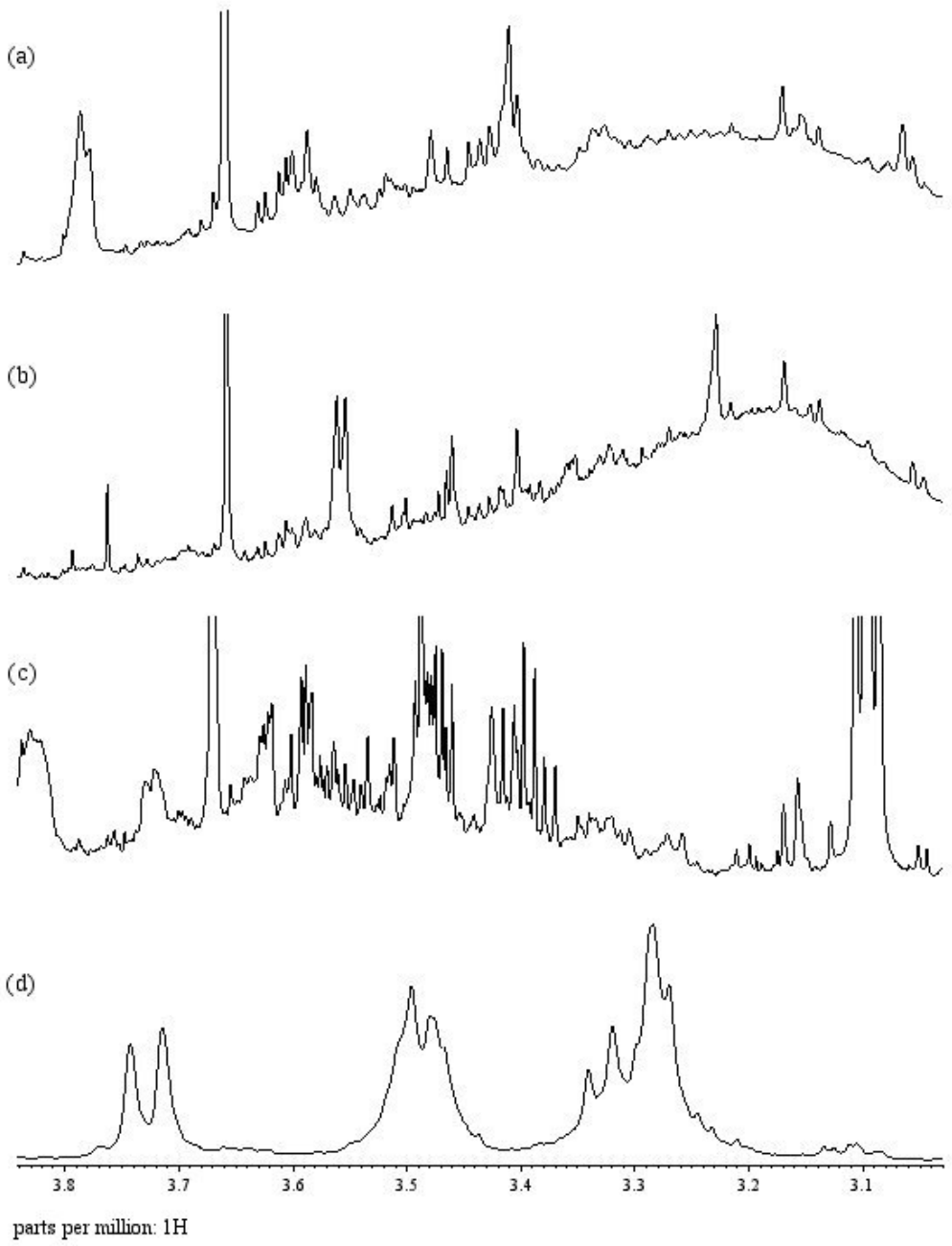

Figure 19. Carbohydrate spectral region from 1H-NMR analysis of liquid urine samples. (a): control urine sample; (b): control urine sample spiked with 2.5 mg/mL glucan; (c): urine sample from the glucan-treated animal; (d): reference sample of pure (1→3)-β-D-glucan.

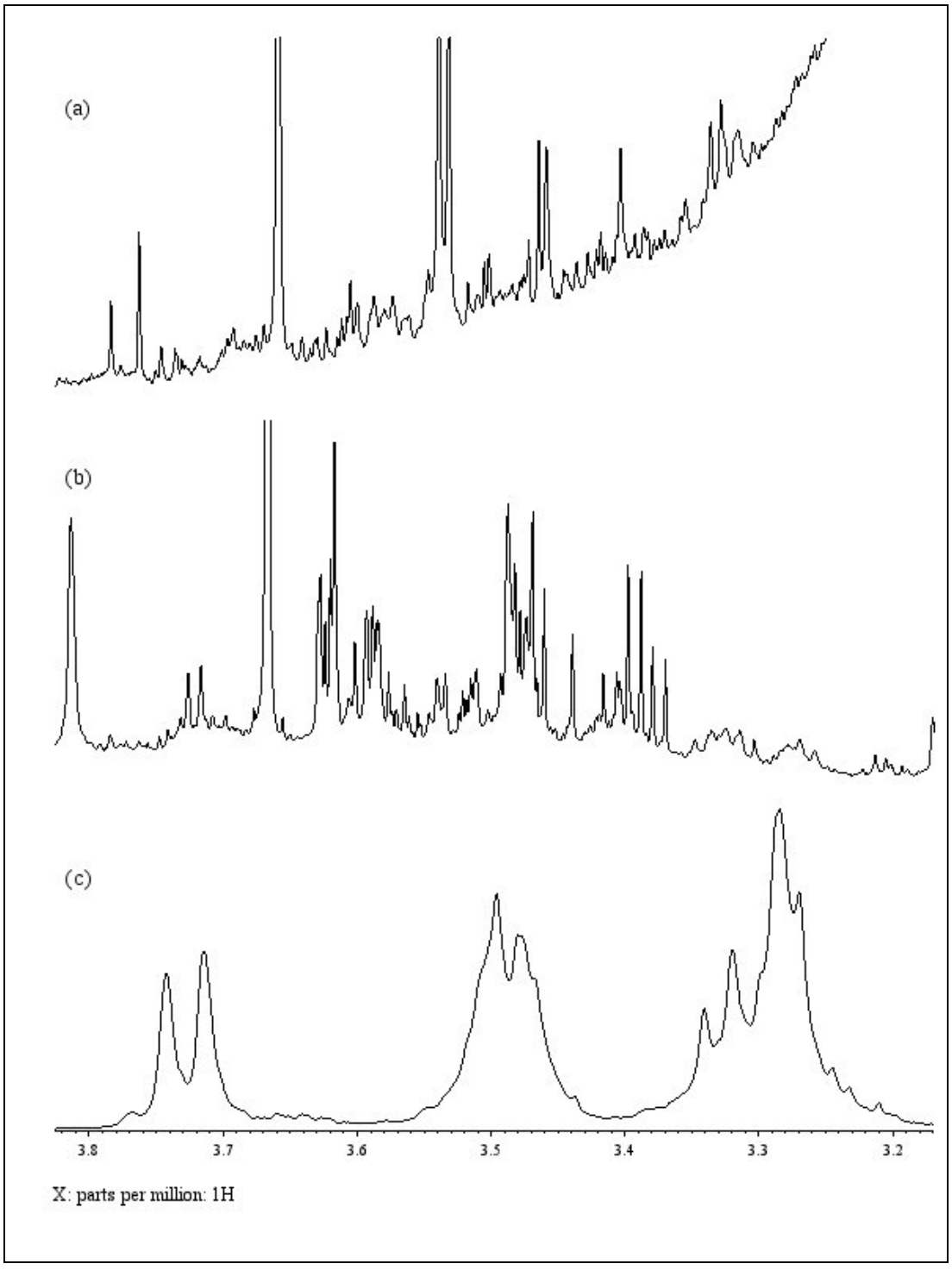

Figure 20. Carbohydrate spectral region from 1H-NMR analysis of lyophilized urine samples. (a): lyophilized control urine sample; (b): lyophilized urine sample from the glucan-treated animal; (c): reference sample of pure (1→3)-β-D-glucan.

Interestingly, upon sample collection from the animal, the urine appeared cloudy; after storage at 40°F overnight, before samples were prepared for NMR analysis, the urine from the treated animal contained a cloudy precipitate appearing to be mid-density with respect to the remainder of the sample (Fig. 21).

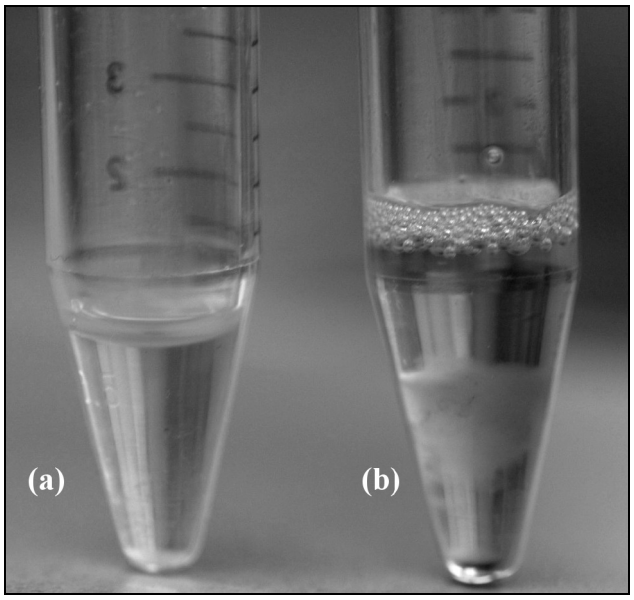

Figure 21. Presence of precipitate in urine from animal treated with unlabeled glucan phosphate for NMR analysis.

In addition to 1H-NMR spectroscopy, a portion of the urine sample containing unlabeled glucan phosphate was submitted for urinalysis to identify the parameters of the sample and to establish possibilities for the precipitate observed in the sample. Results were unremarkable and did not provide any identity for the precipitate (data not shown).

Presence of Fluorescent Glucans in Whole Tissue

To determine if glucans were being trapped within the kidneys, we submitted kidneys from one animal following intravenous glucan phosphate administration for histological slide preparation and counterstaining. Various tissue fixation and mounting methods were employed

to determine if fluorescent glucans were present in the tissue sections; one fixative was used per tissue sample. When sections were examined by fluorescence microscopy, no fluorescence was detected above background level in any of the sections; however, this is not conclusive. We believe there may be two possibilities for our observations: the fixatives used may have caused the glucans to leach out of the tissues prior to fixation and staining, or the glucans are not being retained within the kidney structure. The latter possibility is more likely because multiple fixatives were tested and no fluorescence was detected in any case.

CHAPTER 4

DISCUSSION

Renal (1→3)-β-D-Glucan Excretion

(1→3)-β-D-Glucans have been investigated in great detail in recent years. Their numerous biological and immunological effects have been characterized as anti-tumor agents and anti-inflammatory substances as well as targets for anti-fungal pharmacologic treatment. The pharmacokinetic profiles of these diverse polymers have been well documented by our laboratory following both intravenous and oral administration. This is the first study, however, to focus on the method of excretion for these polysaccharides.

It is evident from the data presented that (1→3)-β-D-glucans are excreted renally. Glucan phosphate, laminarin, and scleroglucan were all detected in the urine following both oral and intravenous administration. Infused laminarin demonstrated significantly high levels of urinary fluorescence, averaging 1253 ± 264 μg/mL. This was followed by injected glucan phosphate, averaging 85 ± 13 μg/mL of fluorescent glucan in the urine; oral glucan phosphate, averaging 49 ± 5 μg/mL of fluorescent glucan in the urine; and injected laminarin and scleroglucan, averaging 30 ± 5 and 33 ± 5 μg/mL of fluorescent urinary glucan, respectively. There is a possibility that the presence of side-chain branching, as seen in laminarin and scleroglucan molecules, may affect the rate or amount of renal glucan excretion; this is supported by the fact that laminarin and scleroglucan demonstrated lower levels of urinary glucans than either intravenous or oral glucan phosphate, even though oral glucan phosphate is known to have a very low bioavailability (0.5%, according to Rice et al. 2005). This observation may also be accounted for by the fact that the animals used in the experiments with injected laminarin and

scleroglucan were of lower body weight than the animals used in the experiments with injected and oral glucan phosphate, influencing the amount of glucan administered.

Following oral administration of glucan phosphate, when compared to intravenously administered glucan phosphate, a lower percentage of the excreted glucans was observed as fragments greater than 5000 Da (53 ± 6% for oral, 66 ± 2% for intravenous). This either signifies that a greater percentage of the oral glucan phosphate was catabolized prior to renal processing, compared to intravenous glucan phosphate; or that the oral glucan phosphate was cleaved into more, and therefore shorter, fragments than the intravenously administered polymer. This difference supports the hypothesis that cleavage of glucan molecules occurs in the intestine prior to or during absorption from the gastrointestinal tract by β-glucan receptors.

Excretion of (1→3)-β-D-glucans appears to be affected in the presence of systemic shock. Lower amounts of total fluorescence were observed in the urine following induction of shock-like state in the animals and oral administration of glucan phosphate, as well as a lower percentage of glucan molecules in the >5000 Da elution fraction: 40 ± 2%, as compared to 53 ± 6% fluorescence in this fraction following oral administration of glucan phosphate in the absence of toxic challenge with LPS. It is unclear at this point what causes the decreased concentration of glucan molecules in the urine with this model, but at least two possibilities exist. First, the small amount of urine in each sample may have precluded reliable detection of fluorescence within the urine, causing abnormally low levels to be observed. Secondly, the lipopolysaccharide-induced shock caused systemic effects, some of which were visible (lethargy, diarrhea) and some of which were internal and therefore not visible. The internal effects may have included decreased absorption of glucan from the gastrointestinal lumen into the bloodstream, decreased metabolism of glucan molecules, or decreased filtration and secretion of

glucan fragments within the nephron; all of these possibilities would have been demonstrated by the low glucan levels detected in the urine.

Possible Catabolism of Glucan Molecules Prior to Excretion

All three polysaccharides, following excretion, were detected as fragments smaller than the molecular size of the administered polysaccharide regardless of administration method. Our size-exclusion chromatography results indicated that 88 ± 1% of intravenous laminarin, 65 ± 2% of intravenous glucan phosphate, 65 ± 11% of intravenous scleroglucan, and 53 ± 6% of oral glucan phosphate were excreted as molecules larger than 5000 Da; in the case of glucan phosphate, these molecules were smaller than the original polymer size as demonstrated by gel permeation chromatography and multi-angle laser light scattering analysis. This observation suggests the possibility of glucan metabolism by the body prior to excretion by the kidneys. The high incidence of molecules larger than 5000 Da within the laminarin sample was not expected. We had theorized that laminarin would demonstrate a smaller percentage of molecules in the first elution fraction; due to the polymer's original size of 7700 Da, cleavage fragments would be more likely to be less than 5000 Da. This finding suggests that laminarin is small enough that it does not require catabolism prior to renal processing but can be filtered into the nephron in its original conformation.

To elucidate whether the process of glucan metabolism occurs, the cellular site of this cleavage must be characterized. (1→3)-β-D-glucans appear to be metabolized elsewhere in the body prior to being transported to the kidneys. At least some of this catabolism appears to occur in the intestines, as supported by the data from the oral glucan experiments and discussed above. Cleavage of glucan molecules would allow for filtration of the smaller fragments through the

glomerular barriers and into the nephron for renal excretion. With the glucan polymers present as smaller molecules, they have not only a lower molecular weight but also a shorter chain structure, giving them increased glomerular permeability. The proposed process of glucan cleavage would require a specific mechanism to drive metabolism of glucan molecules, such as one or more cellular cleavage mechanisms that recognize a specific sequence within the glucan molecule.

Filtration and Secretion of (1→3)-β-D-Glucans

From the introduction, recall that renal filtration of proteins and similar molecules is restricted by molecular size barriers in the peritubular capillary wall. The globular nature of proteins hinders their ability to pass through these pores. However, Asgeirsson et al. (2007) reported that polysaccharides such as dextrans and glucans are more likely to be filtered, due to their linear structure, even though their molecular size may rival that of globular proteins. Laminarin, with its relatively small molecular weight of 7700 Da, is theoretically able to be freely filtered through the peritubular capillary wall of the glomerulus. In contrast, with a molecular weight of approximately 1,000,000 Da, scleroglucan is much too large and long a polysaccharide to be able to pass through this barrier. Glucan phosphate, at 157,000 Da, falls between these two polymers in terms of molecular size and may be permeable to the glomerular barriers in its original form, but this is not proven. If large polysaccharides such as scleroglucan (and possibly glucan phosphate) are to be excreted, as seen by the data presented here, they must be either catabolized into smaller fragments that will not be hindered by the pore size in the capillary epithelium, as discussed above, or secreted into the lumen of the nephron by facilitated diffusion. As a comparison, consider albumin, a plasma protein with a molecular weight of

69,000 Da. Albumin is filtered into the glomerulus, then reabsorbed in the proximal tubule of the nephron only by binding to a protein complex on proximal tubule cells and initiating the endocytosis process (Lazzara and Deen, 2007). A mechanism similar to that of albumin reabsorption may be responsible for glucan secretion into the tubular lumen for urinary excretion and would likely involve previously-identified (1→3)-β-glucan receptors. These receptors, including Dectin-1 and scavenger receptor A, have been identified and characterized by multiple research laboratories. It is widely accepted that these specific receptors exist on cells of the innate immune system, such as macrophages and neutrophils, as well as select non-immune cellular sites including vascular endothelium. Results from our studies support the existence of these or similar β-glucan-specific receptors within the nephron to facilitate diffusion of unfiltered glucans and glucan fragments into the lumen for urinary excretion.

Presence of Glucan Structure in Urine

Results from nuclear magnetic resonance spectroscopy showed no clear evidence regarding the presence of glucan in urine following intravenous administration. The glucan phosphate structure could not be definitively identified in the urine sample from the treated animal. However, this structure also could not be identified in the control urine sample that had been spiked with pure glucan phosphate prior to NMR analysis, suggesting this method may not be a reliable assay for detecting renally excreted glucans. The glucan-specific NMR method has previously been used for identification and characterization of glucans within solution or within a matrix but not for glucan identification within clinical samples. It is not clear why NMR could not detect the glucan structure in the urine samples, even the intentionally spiked sample, contradicting all other experimental results in this study which show the excretion of glucans into

the urine. Therefore, this result neither supports nor refutes the evidence shown in the experiments performed.

Conclusions

We have confirmed that (1→3)-β-D-glucans are excreted into the urine following intravenous and oral administration. Our data corroborate a pharmacokinetic profile involving metabolism of glucan polymers prior to arrival in the nephron, where they are filtered or possibly secreted into the tubular lumen and excreted within the urine. The results we present have significance in both the research and clinical arenas.

The data we present supporting renal excretion of β-glucans open a new area of glucan pharmacokinetics to be investigated: the parameters of excretion of (1→3)-β-D-glucans, including renal clearance and biotransformation. With this information, a complete pharmacokinetic profile of three synthetic glucans - glucan phosphate, laminarin, and scleroglucan - could be compiled and used in the development and use of glucans for clinical application as anti-inflammatory or anti-tumor agents. Secondly, understanding how glucans are handled within the body could also aid in the refinement of serum tests and development of urine tests for fungal infection. Knowing that certain fungal strains shed β-glucans into the bloodstream as they multiply and spread systemically, and knowing from the data presented here that β-glucans are eventually excreted in the urine, clinical urine assays for fungal infection similar to the serum G-test could be developed. Also, identification and characterization of potential β-glucan-specific receptors within the kidney structure would not only lead to a better comprehension of how glucans are handled within the renal system but would also provide new prospective targets for anti-fungal pharmacologic treatments. Similarly, elucidating the

mechanism responsible for cleavage of β-glucan molecules would present another potential anti-fungal therapeutic target. Our data provide a better understanding of (1→3)-β-D-glucan handling within the body and supply the groundwork necessary for further glucan research and development.

REFERENCES

Adams EL, Rice PJ, Graves B, Ensley HE, Yu H, Brown GD, Gordon S, Monteiro MA, Papp-Szabo E, Lowman DW, Power TD, Wempe MF and Williams DL (2008) Differential high affinity interaction of dectin-1 with natural or synthetic glucans is dependent upon primary structure and is influenced by polymer chain length and side chain branching. *J Pharmacol Exp Ther*. **325:**115-23.

Ahren IL, Williams DL, Rice PJ, Forsgren A and Riesbeck K (2001) The importance of the β-glucan receptor in the nonopsonic entry of nontypeable *Haemophilus influenzae* into human monocytic and epithelial cells. *J Infect Dis.* **184:**150-158.

Asgeirsson D, Venturoli D, Fries E, Rippe B and Rippe C (2007) Glomerular seiving of three neutral polysaccharides, polyethylene oxide and bikunin in rat: effects of molecular size and conformation. *Acta Physiol* **191:** 237-246.

Breuel KF, Kougias P, Rice PJ, Wei D, De Ponti K, Wang J, Laffan JJ, Li C, Kalbfleisch J and Williams DL (2004) Anterior pituitary cells express pattern recognition receptors for fungal glucans: implications for neuroendocrine immune involvement in response to fungal infections. *Neuroimmunomodulation* **11:**1-9.

Brown GD and Gordon S (2001) Immune recognition: a new receptor for beta-glucans. *Nature* **413:**36-37.

Brown GD, Taylor PR, Reid DM, Willment JA, Williams DL, Martinez-Pomares L, Wong SY, Gordon S (2002) Dectin-1 is a major beta-glucan receptor on macrophages. *J Exp Med.* **196:**407-412.

Brown GD, Herre J, Williams DL, Willment JA, Marshall ASJ and Gordon S (2003) Dectin-1 mediates the biological effects of β-glucans. *J Exp Med.* **197:**1119-1124.

Brown GD and Gordon S (2003) Fungal β-glucans and mammalian immunity. *Immunity* **19:**311-315.

Costanzo LS (2006) Renal physiology, in *Physiology*, 3rd ed, pp. 207-264, W.B. Saunders, Philadelphia.

Czop JK and Austen KF (1985) A beta-glucan inhibitable receptor on human monocytes: its identity with the phagocytic receptor for particulate activators of the alternative complement pathway. *J Immunol.* **134:**2588-93.

Digby J, Kalbfleisch J, Glenn A, Larsen A, Browder W and Williams D (2003) Serum glucan levels are not specific for presence of fungal infections in intensive care unit patients. *Clin Diagn Lab Immunol.* **10:**882-5.

Douglas CM (2001) Fungal β(1,3)-D-glucan synthesis. *Med Mycol.* **39** (Suppl. 1):55-66.

Ensley HE, Tobias B, Pretus HA, McNamee RB, Jones EL, Browder IW and Williams DL (1994) NMR spectral analysis of a water-insoluble (1→3)-β-D-glucan isolated from *Saccharomyces cerevisiae*. *Carbohyd Res.* **258:**307-311.

Herre J, Marshall ASJ, Caron E, Edwards AD, Williams DL, Schweighoffer E, Tybulewicz V, Reis e Sousa C, Gordon S and Brown GD (2004) Dectin-1 uses novel mechanisms for yeast phagocytosis in macrophages. *Blood* **104:**4038-4045.

Hong F, Hansen RD, Yan J, Allendorf DJ, Baran JT, Ostroff GR and Ross GD (2003) β-Glucan functions as an adjuvant for monoclonal antibody immunotherapy by recruiting tumoricidal granulocytes as killer cells. *Cancer Res.* **63:**9023-31.

Hong F, Yan J, Baran JT, Allendorf DJ, Hansen RD, Ostroff GR, Xing PX, Cheung N-KV, Ross GD (2004) Mechanism by which orally administered β-1,3-glucans enhance the tumoricidal activity of antitumor monoclonal antibodies in murine tumor models. *J Immunol.* **173:**797-806.

Kim YT, Kim E, Cheong C, Williams DL, Kim CW and Lim ST (2000) Structural characterization of β-D-(1→3, 1→6) glucans using NMR spectroscopy. *Carbohyd Res.* **328:**331-341.

Kougias P, Wei D, Rice PJ, Ensley HE, Kalbfleisch J, Williams DL, and Browder IW (2001) Normal human fibroblasts express pattern recognition receptors for fungal (1→3)-β-D-glucans. *Infection and Immunity* **69:**3933-3938.

Kulicke WM, Lettau AI and Thielking H (1997) Correlation between immunological activity, molar mass, and molecular structure of different (1-->3)-beta-D-glucans. *Carbohydr Res.* **297:**135-43.

Lazzara MJ, Deen WM (2007) Model of albumin reabsorption in the proximal tubule. *Am J Physiol Renal Physiol.* **292:**F430-9.

Lowe EP, Wei D, Rice PJ, Li C, Kalbfleisch J, Browder IW and Williams DL (2002) Human vascular endothelial cells express pattern recognition receptors for fungal glucans which stimulates nuclear factor κB activation and interleukin 8 production. *Am Surg.* **68:**508-517.

Lowman DW and Williams DL (2001) A proton nuclear magnetic resonance method for the quantitative analysis on a dry weight basis of (1→3)-β-D-glucans in a complex, solvent-wet matrix. *J Agric Food Chem.* **49:**4188-91.

Lowman DW, Ferguson DA and Williams DL (2003) Structural characterization of (1→3)-β-D-glucans isolated from blastospore and hyphal forms of Candida albicans. *Carbohydr Res*. **338:**1491-6.

Miyazaki T, Kohno S, Mitsutake K, Maesaki S, Tanaka K, Ishikawa N and Hara K (1995) Plasma (1→3)-β-D-glucan and fungal antigenemia in patients with candidemia, aspergillosis, and cryptococcosis. *J Clin Microbiol.* **33:**3115-18.

Moghaddam B and Bunney B (1989) Ionic composition of microdialysis perfusing solution alters the pharmacological responsiveness and basal outflow of striatal dopamine. *J Neurochem*. **53:**652-4.

Mueller A, Raptis J, Rice PJ, Kalbfleisch JH, Stout RD, Ensley HE, Browder W and Williams DL (2000) The influence of glucan polymer structure and solution conformation on binding to (1→3)-β-D-glucan receptors in a human monocyte-like cell line. *Glycobiology* **10:**339-346.

Obayashi T, Yoshida M, Mori T, Goto H, Yasuoka A, Iwasaki H, Teshima H, Kohno S, Horiuchi A, Ito A, et al (1995) Plasma (1→3)-β-D-glucan measurement in diagnosis of invasive deep mycosis and fungal febrile episodes. *Lancet* **345:**17-20.

Obayashi T, Negishi K, Suzuki T and Funata N (2008) Reappraisal of the serum (1-->3)-beta-D-glucan assay for the diagnosis of invasive fungal infections--a study based on autopsy cases from 6 years. *Clin Infect Dis.* **46:**1864-70.

Onishi J, Meinz M, Thompson J, Curotto J, Dreikorn S, Rosenbach M, Douglas C, Abruzzo G, Flattery A, Kong L, Cabello A, Vicente F, Pelaez F, Diez MT, Martin I, Bills G, Giacobbe R, Dombrowski A, Schwartz R, Morris S, Harris G, Tsipouras A, Wilson K, Kurtz MB (2000) Discovery of novel antifungal (1,3)-beta-D-glucan synthase inhibitors. *Antimicrob Agents Chemother.* **44:**368-377.

Pretus HA, Ensley HE, McNamee RB, Jones EL, Browder IW and Williams DL (1991) Isolation, physicochemical characterization and preclinical efficacy evaluation of soluble scleroglucan. *J Pharmacol Exp Ther.* **257:**500-510.

Reusch W (1991) NMR spectroscopy. Revised 10 August 2007. Retrieved 8 July 2008 from http://www.cem.msu.edu/~reusch/VirtualText/Spectrpy/nmr/nmr1.htm

Rice PJ, Kelley JL, Kogan G, Ensley HE, Kalbfleisch JH, Browder IW and Williams DL (2002) Human monocyte scavenger receptors are pattern recognition receptors for (1→3)-β-D-glucans. *J Leukoc Biol.* **72:**140-146.

Rice PJ, Lockhart BE, Barker LA, Adams EL, Ensley HE and Williams DL (2004) Pharmacokinetics of fungal (1-3)-beta-D-glucans following intravenous administration in rats. *Int Immunopharmacol.* **4:**1209-15.

Rice PJ, Adams EL, Ozment-Skelton T, Gonzalez AJ, Goldman MP, Lockhart BE, Barker LA, Breuel KF, DePonti WK, Kalbfleisch JH, Ensley HE, Brown GD, Gordon S and Williams DL (2005) Oral delivery and gastrointestinal absorption of soluble glucans stimulate increased resistance to infectious challenge. *J Pharmacol Exp Ther.* **314:**1079-1086.

Ross GD, Cain JA, Myones BL, Newman SL and Lachmann PJ (1987) Specificity of membrane complement receptor type three (CR3) for beta-glucans. *Complement* **4:**61-74.

Sletmoen M and Stokke BT (2008) Higher order structure of (1,3)-β-D-glucans and its influence on their biological activities and complexation abilities. *Biopolymers* **89:**310-321.

Thornton BP, Větvicka V, Pitman M, Goldman RC and Ross GD (1996) Analysis of the sugar specificity and molecular location of the beta-glucan-binding lectin site of complement receptor type 3 (CD11b/CD18). *J Immunol.* **156:**1235-1246.

Větvicka V, Thornton BP and Ross GD (1996) Soluble β-glucan polysaccharide binding to the lectin site of neutrophil or NK cell complement receptor type 3 (CD11b/CD18) generates a primed state of the receptor capable of mediating cytotoxicity of iC3b-opsonized target cells. *J Clin Investig*. **98:**50-61.

Williams DL, McNamee RB, Jones EL, Pretus HA, Ensley HE, Browder IW and Di Luzio NR (1991) A method for the solubilization of a (1→3)-β-D-glucan isolated from *Saccharomyces cerevisiae*. *Carbohyd Res.* **219:**203-213.

Williams DL, Rice PJ, Herre J, Willment JA, Taylor PR, Gordon S and Brown GD (2003) Recognition of fungal glucans by pattern recognition receptors. *Recent Devel Carbohydrate Res.* **1:**49-66.

VITA

DEBRA K. HEAD

Personal Data:	Date of Birth: March 18, 1983 Place of Birth: Indianapolis, Indiana
Education:	Public Schools, Plainfield, Indiana 1988-2001 B.S. Biology, Milligan College, Milligan College, Tennessee 2005 M.S. Biomedical Science/Pharmacology, East Tennessee State University, Johnson City, Tennessee 2008
Professional Experience:	Laboratory Assistant and Tutor, Milligan College, Department of Biology, 2003-2005, 2008- Anatomic Pathology Technician, Highlands Pathology Consultants, Kingsport, Tennessee, 2005- Graduate Research Assistant, East Tennessee State University, Department of Pharmacology, 2006-2008
Presentations:	Urinary excretion of fungal (1-3)-β-D-glucan phosphate following IV administration. Poster. Appalachian Student Research Forum, East Tennessee State University, 2008. Urinary excretion of fungal (1-3)-β-D-glucan phosphate following IV administration. Poster. American Society for Microbiology general meeting, Boston, Massachusetts, 2008.